Host–guest interactions in framework materials

Ernst, Michelle; Evans, Jack D.; Gryn'ova, Ganna

[Link to publication on Research at Birmingham portal](#)

Host–guest interactions in framework materials: Insight from modeling ⓕ

Michelle Ernst ⓘ ; Jack D. Evans ⓘ ; Ganna Gryn'ova ✉ ⓘ

Check for updates

View Online

Export Citation

Host–guest interactions in framework materials: Insight from modeling ⓕ

Michelle Ernst,[1,2] ⓘ Jack D. Evans,[3] ⓘ and Ganna Gryn'ova[1,2,a] ⓘ

AFFILIATIONS

[1]Heidelberg Institute for Theoretical Studies (HITS gGmbH), Schloss-Wolfsbrunnenweg 35, Heidelberg 69118, Germany
[2]Interdisciplinary Center for Scientific Computing, Heidelberg University, Im Neuenheimer Feld 205, Heidelberg 69120, Germany
[3]Centre for Advanced Nanomaterials and Department of Chemistry, The University of Adelaide, North Terrace, Adelaide, South Australia 5000, Australia

[a]Author to whom correspondence should be addressed: ganna.grynova@h-its.org

ABSTRACT

The performance of metal–organic and covalent organic framework materials in sought-after applications—capture, storage, and delivery of gases and molecules, and separation of their mixtures—heavily depends on the host–guest interactions established inside the pores of these materials. Computational modeling provides information about the structures of these host–guest complexes and the strength and nature of the interactions present at a level of detail and precision that is often unobtainable from experiment. In this Review, we summarize the key simulation techniques spanning from molecular dynamics and Monte Carlo methods to correlate *ab initio* approaches and energy, density, and wavefunction partitioning schemes. We provide illustrative literature examples of their uses in analyzing and designing organic framework hosts. We also describe modern approaches to the high-throughput screening of thousands of existing and hypothetical metal–organic frameworks (MOFs) and covalent organic frameworks (COFs) and emerging machine learning techniques for predicting their properties and performances. Finally, we discuss the key methodological challenges on the path toward computation-driven design and reliable prediction of high-performing MOF and COF adsorbents and catalysts and suggest possible solutions and future directions in this exciting field of computational materials science.

TABLE OF CONTENTS

I. INTRODUCTION

At a first glance, it may appear that water filtration with activated carbon, sound absorption with metal foams, and water softening using zeolites in laundry detergents have very little in common. However, all these processes rely on materials possessing tiny pores—microporous materials—with diameters in the nanometer range, which is less than the wavelength of visible light.

Naturally occurring porous materials have been used for a long time. For example, charcoal is a naturally porous substance, known to and used by the ancient Egyptians, Greeks, and Romans.[1] In the *Naturalis Historia*, Pliny the Elder describes the utility of charcoal in the treatment of "carbuncles." (A carbuncle is a cluster of boils that

form a connected area of infection under the skin.) Nowadays, charcoal is still used in various beauty products. In 1854, John Stenhouse invented face masks employing charcoal to filter the air, which proved to be useful in hospitals.[2] Since those early discoveries, numerous porous materials have been developed and manufactured artificially to address a range of laboratory and industrial needs.

Owing to their structural and compositional diversity and tunability of physical and chemical properties, metal–organic frameworks (MOFs) and covalent organic frameworks (COFs) are particularly promising candidates for various applications requiring microporous materials. MOFs are constructed from polynuclear metal-containing building units (called secondary building units, or SBUs) joined by organic linkers into various network topologies. Since demonstrating permanent porosity in 1994 by Yaghi *et al.*,[3] MOFs have continuously attracted the attention of researchers worldwide. COFs are promising organic analogues of MOFs, first described in 2005[4] and consisting of elements typical for organic molecules. The ability of MOFs and COFs to capture, store, and release guest molecules is, arguably, their most prominent feature, exploited in gas storage,[5–7] gas separation,[8,9] energy storage,[10] gas adsorption,[11–13] catalysis,[14–17] sensing,[18–20] and biomedical applications.[21,22] The nature, behavior, and quantity of absorption depend on pore size and volume, surface area, chemical environment, and, in particular, on the host–guest intermolecular interactions.

The ultimate goal of all efforts in materials science is to make better materials, either through the discovery of new or the improvement and repurposing of existing systems. *In silico* modeling facilitates these efforts by elucidating the fundamental mechanisms of action and establishing the structure–property relationships. An extensive review by Mancuso *et al.*[23] discusses general electronic structure approaches to modeling metal–organic frameworks, while Gagliardi and co-workers discuss modeling techniques of MOFs for catalytic applications with particular focus on natural gas conversion.[24] In 2015, Lee *et al.* published an insightful overview article on studying the small-molecule interactions in MOFs by combined theoretical and experimental approaches.[25] More recently, Qiao and co-workers traced the transition from single simulations to high-throughput screening (HTS) and machine learning of MOF adsorbents.[26] In this Review, we focus more narrowly on the computational studies of the host–guest complexes between framework materials and their molecular targets, exemplifying common simulation techniques and discussing their advantages and shortcomings. The diversity of framework materials and their applications requires simulations at various time and lengths scales. If the objective is an overview of an entire system containing thousands of atoms, atomistic methods based on parametrized force fields are the preferred, albeit less precise choice. Electronic structure methods not only offer more accurate but also more costly means to identify specific adsorption sites and quantify the host–guest interactions (HGIs). These approaches, either used independently or combined in a multiscale manner, are general and can be applied to study host–guest interactions in other crystalline and porous materials, such as zeolites. Finally, up-and-coming machine learning techniques coupled with high-throughput data generation allow rapid screening of thousands of existing and hypothetical frameworks.

II. ZONE DEFENSE: DYNAMIC BEHAVIOR

The playing field that is comprised by the pore space within framework materials is a battleground for guests to follow trajectories related to adsorption/desorption and diffusion. These processes, in unison, are responsible for the observed performance in guest separation and storage. For example, a membrane's separation performance is dictated by permeability, which is the product of diffusivity and concentration, in turn related to diffusion and adsorption, respectively.[27] The processes of diffusion and adsorption appear intertwined but they relate to distinct temporal domains: diffusion is a kinetic property, and adsorption is an equilibrium property. As a result, distinct computational strategies are often employed to examine each of these processes.[28–33]

Throughout the literature, diffusivity is usually treated with molecular dynamics (MD) simulations that sample the trajectories of guests by solving equations of motion for the particles within the system, including the forces and potential energies between particles.[34] We note that diffusion can also be estimated by Monte Carlo (MC) simulations and transition state theory.[35] Simulating the potential energy and forces for this application is achieved using classical approaches to treating guest–guest and guest–framework interactions that accelerate the simulations permitting the simulation over long time scales (>1 ns), required to accurately describe statistics of diffusion processes. Molecular diffusion in fully flexible models, where both the guest and the pore walls move, is preferred but only if a suitable force field is available. A force field is a mathematical model that describes the interactions between atoms or molecules, and it is crucial for the accuracy of MD simulations. In recent years, a number of force fields have been developed specifically for MOFs. One example of a force field that has been shown to be effective for MOFs is the ZIF-8 force field developed by Zhang *et al.*[36] Similarly, Wu *et al.* used a bespoke force field to simulate CO_2 transport diffusion in UiO-66 and reported a value in good agreement with experimental data.[37] It is important to note that these bespoke force fields are usually not applicable to other materials. Force fields are constantly improved by the community and can be derived from *ab initio* data.[38] In order to overcome this limitation, several force fields have been introduced in recent years that are more universal in their applicability. One such example is the universal force field for MOFs (UFF4MOF), which is based on a universal force field for small molecules.[39] Addicoat *et al.*[40] and Coupry *et al.*[41] supplemented the original universal force field by adding new atom types for metal elements to better describe the coordinate bonds in MOFs. With the recent development of more universal force fields for MOFs, it is becoming possible to study diffusion in a wider range of materials using MD simulations.

The key quantity measured throughout the molecular dynamics trajectories is the mean squared displacement of the individual guests moving throughout the structure. From the mean squared displacements, the self-diffusivity (in three-dimensions) can be computed in an analogous way to experiments:[42]

$$D_{\text{self}} = \frac{1}{6} \lim_{t \to \infty} \frac{d}{dt} \left\langle \left| \boldsymbol{r}(t) - \boldsymbol{r}(0) \right|^2 \right\rangle. \tag{1}$$

Computing self-diffusivity from molecular dynamics trajectories does require careful analysis to ensure sufficient sampling of diffusion events. For example, the simulated diffusivity of several gases in MOF-5 demonstrates that the magnitude of diffusivity is related to the properties of the guest [Fig. 1(a)].[43,44] Self-diffusivity is a useful measure of diffusion capturing both guest–guest and guest–framework collisions and enabling a close comparison with experiment, provided an accurate fully flexible model is used for the guests and framework.[45]
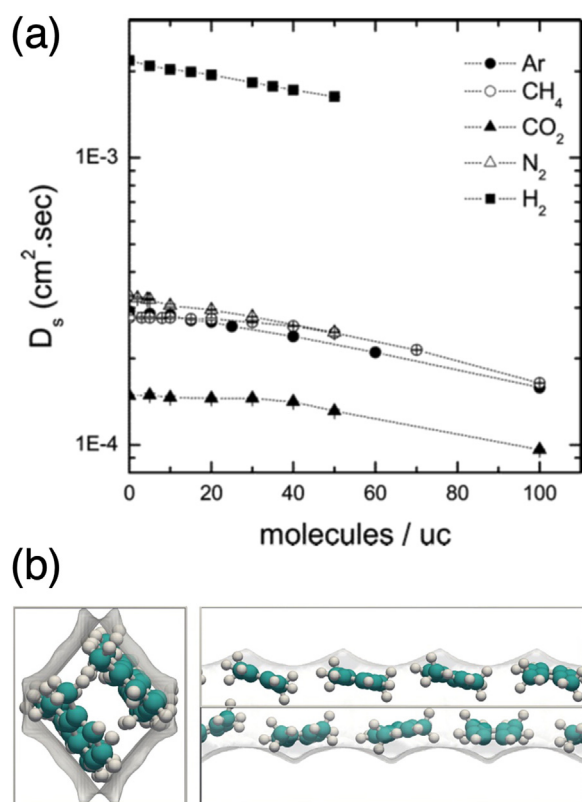
FIG. 1. (a) Simulated self-diffusivities of various gases in MOF-5 at room temperature. Reproduced with permission from A. I. Skoulidas and D. S. Sholl, J. Phys. Chem. B **109**, 15760 (2005). Copyright 2005 American Chemical Society.[44] (b) Snapshot of GCMC simulation of *o*-xylene packing in MIL-47 at 433 K, (left) view along the channel, (right) side view with the channel 45° rotated around the channel axis (the line in the center is an edge of the unit cell). Reproduced with permission from Knoop *et al.*, Mol. Simul. **42**, 81 (2016). Copyright 2016 Authors, licensed under a Creative Commons Attribution-NonCommercial-NoDerivatives (CC BY NC ND) license.[46]

Adsorption at very low pressures, for example in the Henry's law regime, can be sampled by completely random sampling to simply capture the guest–framework interactions. This random sampling is employed by Monte Carlo (MC)—a method that focuses on static properties of systems and does not involve the evolution of systems over time. In contrast to molecular dynamics (MD), where each state of the system depends on the previous state, in MC, there is no connection between the snapshots (states) of the system. Most MC algorithms are based on modifying the current snapshot by performing changes called "moves" and using an "acceptance rule" to determine whether the new state should be accepted or rejected. However, MC is rarely applied to chemically complex molecules and frameworks and has a reputation for being difficult to debug and test. The RASPA software is a general purpose classical simulation package for MC and is used throughout the literature.[46] MC can uncover the interaction strength for the guest in the framework. However, more complex MC moves correctly sampling the thermodynamics, such as grand canonical Monte Carlo (GCMC) simulations, are necessary to compute the loading of guest at a specific pressure, in order to simulate an isotherm.[47] Configurational bias GCMC can be employed to simulate the flexibility of guests.[48] In general, Monte Carlo simulations involve the sampling of millions of moves that include trial displacement, insertion, and removal of guest molecules in the framework structure. The number of guests adsorbed in framework will evolve over the course of GCMC simulation, and after a period of equilibration, it will fluctuate around an equilibrium value.[46,49] Snapshots from GCMC simulations are useful to demonstrate how guests may pack in the porous space [Fig. 1(b)]. This equilibrium imitates the experimental system, in which the adsorbed phase is at equilibrium with a gas reservoir. These approaches allow for the system configuration to sample the equilibrium case that cannot be sampled efficiently through molecular dynamics simulations.

For even more rigorous quantitative insights, traditional molecular dynamics simulations can be combined with *ab initio* modeling, e.g., at the density functional theory (DFT) level, to simultaneously sample configurational space, describe the electronic structure of the host–guest complexes, as well as take into account entropic and enthalpic effects.[50–53] This approach is described as *ab initio* molecular dynamics (AIMD) and is the most accurate method to study the dynamic behavior of guest molecules in porous materials. With this approach, one can establish a relation between the electronics of the host–guest system and its macroscopic properties. It is also well-suited to treat solid–liquid interfaces. However, AIMD is extremely computationally intensive, and this often results in limited sampling. Consequently, AIMD has not been widely applied to guest molecules in MOFs and COFs, apart from a few notable exceptions where it was employed to (i) model the uptake and release of gases, determine its temperature dependence and its effect on structural and electronic properties of MOFs;[54–57] (ii) model breathing and structural flexibility upon adsorption;[58–62] (iii) study the degradation and formation of MOFs in water;[63–67] (iv) investigate proton conduction of guests in MIL-53;[68] and (v) study ferroelectricity and how it is influenced by trapped water molecules.[69]

III. ONE-ON-ONE: STATIC BEHAVIOR

The nature and strength of the interactions, established upon the guest's diffusion and adsorption in the host's pore, often determine—and can, therefore, be exploited to tune—the selectivity and efficacy of the framework material used to capture, separate, catalytically activate, and/or transport small molecules. These HGIs occasionally involve covalent bonding, but are more commonly non-covalent (intermolecular), spanning from very strong interactions (e.g., hydrogen or dative bonds to metal atoms in MOFs) to relatively weak interactions (e.g., van der Waals forces as is the case of inert gases). We note that dispersion interactions are the dominate energy contribution to most HGIs at the short range.

Accurate *in silico* characterization of the host–guest complexes generally relies on electronic structure theory in a "so-called" static setting, in which single-point computations are performed on either an equilibrium structure (partially or fully relaxed) or on an experimental structure. The choice of the simulation technique is often guided by the requirements of a specific application: the relative adsorption strengths of different guests are critical for separation processes, the exact location and structure of a guest are important for a catalytic mechanism, and the host–guest interaction type is central to sensing. Practical applications of framework materials vary depending on the

size of the molecular guest relative to the pore space. Small guests are molecules made up of only a few atoms and occupying a relatively small portion of the pore volume. Typical examples include gaseous molecules, such as H_2, N_2, O_2, CO_2, H_2O, and light hydrocarbons, e.g., methane, ethane, ethylene, etc. For these small guests, framework materials, owing to their controllable and adjustable porosity, structure, and surface functionalities, are utilized primarily to separate mixtures (such as ethane and ethylene, methane and CO_2, O_2, and N_2, etc.), as well as for capture (particularly CO_2) and storage (e.g., H_2).[6,8] Larger guests, such as drug molecules, are typically dissolved in solvents and loaded together with the solvent. Their applications often involve MOFs for catalysis, drug delivery, and sensing.[9,24,70] Since these guest can form more and stronger interactions with the framework, a detailed analysis of these interactions becomes critical.

Two types of structural models are usually considered: periodic and finite (cluster) models. Periodic computations account for the crystalline (periodic in three dimensions) nature of the material, but are computationally demanding, and therefore, often restricted to density functional theory. In contrast, finite models (clusters), cut out from the periodic structure and capped with (most commonly) hydrogen atoms, can be treated not only at the DFT but also at correlated wavefunction theory levels, such as coupled cluster and perturbation theory. Choosing a model is a balancing act between the precision of the computational method and that of the structural model.

A. Periodic computations

Periodic approaches often use density functional theory methods from the lower rungs on the Jacob's ladder, such as the local density approximation (LDA) and generalized gradient approximation (GGA). These methods by construction lack the description of dispersion, crucial in the host–guest interactions.[71] To remedy this shortcoming and achieve agreement with the experimental data, either the empirical dispersion corrections, such as Grimme's D2 and D3 featuring the R^6 term[72] are added to the "bare" DFT results, or the so-called van der Waals (vdW) DFT functionals,[73] which self-consistently account for dispersion through non-local correlation, are employed. Siegel and co-workers benchmarked these methods against experimental enthalpies of CO_2 adsorption in four prototypical metal–organic frameworks: M/DOBDC (M = Mg, Ni, and Co) and 5Cu-HKUST-1.[74] LDA methods alone were found to significantly overbind, and GGA—to underbind carbon dioxide; addition of D2 dispersion correction notably improved these results both qualitatively and quantitatively, albeit still underestimating the CO_2 adsorption enthalpies by *ca.* 7 kJ mol^{-1} compared to experiment. Nonempirical vdW density functionals, particularly revPBE, afforded the best agreement (within ~2 kJ mol^{-1}) with the reference experimental data (Fig. 2). The same authors later expanded the range of the studied metal atoms in the two MOFs, i.e., M-DOBDC with M = Mg, Ca, Sr, Sc, Ti, V, Mo, and W, and M-HKUST-1 with M = Be, Mg, Ca, Sr, and Sc, reaching very similar conclusions regarding the DFT performance.[75]

LDA and GGA functionals also lack a proper description of the strong on-site Coulomb interaction of localized *d*-electrons of metal atoms. This is especially important for open metal sites (OMSs), which are formed when solvent is removed from a crystalline metal–organic framework, and which largely define the interactions with the guest molecules. To address this issue, DFT methods are appended with an additional Hubbard term and are consequently denoted as DFT + U approaches.[76] Investigating the interactions of isostructural metal–organic frameworks based on M-MOF-74 (where M = Mg, Ti, V, Cr, Mn, Fe, Co, Ni, Cu, and Zn) with various gaseous and small hydrocarbon molecules (including H_2, CO_2, N_2, H_2O, H_2S, NH_3, CH_4, C_2H_4, etc.), Lee *et al.* demonstrated that the Hubbard U corrections are necessary to correctly predict not only of the ground-state multiplicity of
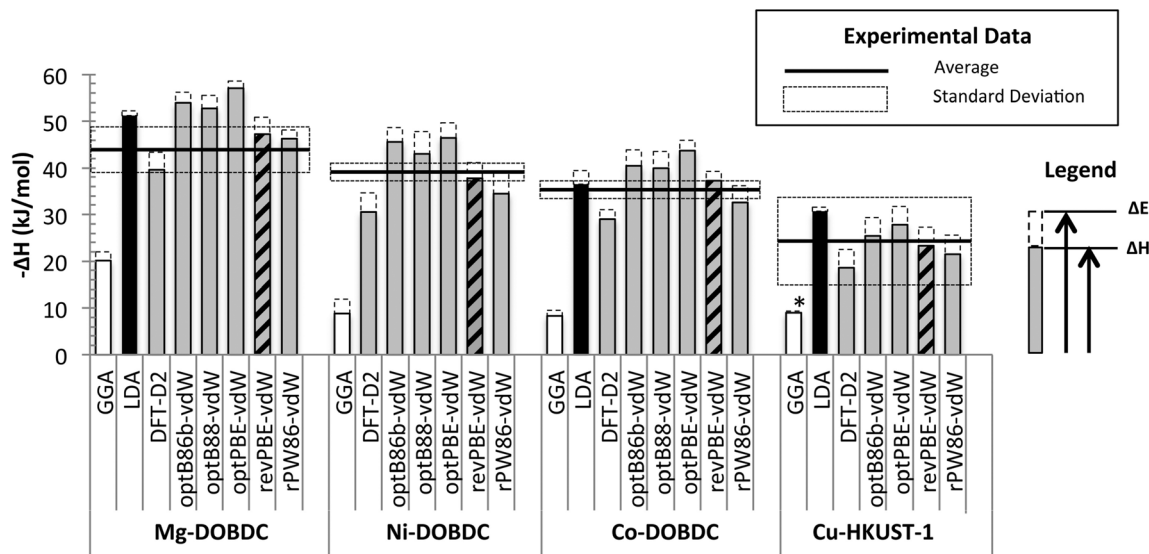
FIG. 2. Performance of various DFT methods for computing CO_2 adsorption energies in M/DOBDC (M = Mg, Ni, Co) and HKUST-1. The total column heights represent the 0 K static binding energy, and the dashed segments at the top indicate the sum of zero-point and thermal energy contributions at 300 K (* denotes this contribution for Cu-HKUST-1 at the PBE-GGA level, equal to −0.5 kJ mol^{-1}). The average experimental ΔH is given as a horizontal line; the standard deviation in the experimental data is given by a dashed box. Reproduced with permission from Rana *et al.*, J. Phys. Chem. C **116**, 16957 (2012). Copyright 2012 American Chemical Society.[74]

the transition metals in MOFs but also of the binding energies in their host–guest complexes.[77] On the other hand, Kim et al. showed that adding Hubbard U-corrections to PBE-D2 binding energies between small hydrocarbons and Fe-MOF-74 significantly worsens their agreement with experiment.[78] This demonstrates the difficulties faced when investigating OMSs.

To reproduce experimental heats of adsorption beyond qualitative trends, zero-point vibrational energy and thermal energy corrections must be added to compute electronic energies of the host–guest binding. This can be achieved by numerical differentiation of the analytical first derivatives to estimate vibrational frequencies. Heats of adsorption of N_2, CO, and CO_2 on Mg-MOF-74, computed in this manner at the B3LYP-D* level of theory, were shown to be in a reasonably good agreement with the data from variable-temperature infrared spectroscopy.[79] Delle Piane et al. demonstrated that dispersion correction is needed to predict spontaneous adsorption of ibuprofen on MOF MCM-41 walls (in accordance with experimental observations), while the lack of dispersion correction lead to positive values of the free energies of adsorption.[80] Vibrational frequencies, computed using a finite-differences approach to obtain a Hessian matrix of second derivatives of the total energy, were used by Lee et al.[77] to assess the quantum nuclear zero-point vibrational energies and finite-temperature thermal energies under the harmonic approximation at the vdW-D2 + U2 level of theory. Figure 3(a) clearly demonstrates the need to include these effects to reproduce experimental heats of adsorption.

While many periodic approaches use ab initio pseudopotentials and plane-waves (such as the projector augmented wave method),[81] a fully periodic hybrid Hartree–Fock/DFT simulation of CO_2 adsorption on MIL-100(MIII) with MIII = Al, Sc, Cr, and Fe using instead atom-centered basis sets was performed by D'Amore et al.[82] Specifically, dispersion-corrected B3LYP and MO6 computations employed a triple-zeta pob-TZVP/6–311G(d,p) basis set on the metal atoms, a 6–311G** Pople basis set on the H, C, and O atoms of the framework, and a TZP basis set on the CO_2 molecule. A massively parallel version of the CRYSTAL code was used in these computations involving over 50 000 basis functions. The computed interaction energies, corrected

for the basis set superposition error, are in reasonable agreement with experiment.

Computed binding energies can be used to assess the performance of diverse MOFs in the separation of gas mixtures. For example, Sholl and co-workers considered the M-BTC framework, where BTC is the 1,3,5-benzenetricarboxylic acid, and M = Mg, Ti, V, Cr, Mo, Mn, Fe, Ru, Co, Ni, Cu, and Zn, for the separation of the water, carbon monoxide, ethane, ethene, and ethyne [Figs. 3(b) and 3(c)], demonstrating a relationship between binding energies and separation efficiencies.[83] Similarly, Cunha et al. rationalized the impact of the ligand functionalization on the release of caffeine from functionalized MIL-53 via binding energies.[84] Furthermore, periodic DFT computations allow elaborating the mechanistic details of, e.g., separation of C_2H_4 and C_2H_6 on ZIF-7,[85] conversion of NO into NO_2 in Mn-MOF-74,[86] fixation of CO_2 in HbMOF1,[87] or catalytic hydrogenation of CO_2 by a Lewis pair functionalized MOF, UiO-66-P-BF_2.[88,89]

Apart from structural and energetic considerations, ab initio modeling allows characterizing the electronic structure of the host–guest complexes in organic frameworks. Bader charge analysis[90] is often employed to establish the oxidation state of the metal node in MOFs, and to rationalize the extent of charge transfer between the framework and the guest.[85,91,92] For example, Canepa et al. suggested that a relationship exists between the charge of the metal ion in M-MOF-74, where M = Be, Mg, Al, Ca, Sc, Ti, V, Cr, Mn, Fe, Co, Ni, Cu, Zn, Sr, Zr, Nb, Ru, Rh, Pd, La, W, Os, Ir, and Pt, and the strength of adsorption of small molecules (H_2, CO_2, CH_4, and H_2O) in its pores.[93] A similar observation was also made by Koh et al. for CO_2 adsorption on M-DOBDC and M-HKUST-1, where M = Be, Mg, Ca, Sr, Sc, Ti, V, Cr, Mn, Fe, Co, Ni, Cu, Zn, Mo, W, Sn, and Pb.[75] These findings put forward the metal ion charge as a potential descriptor of adsorption energy for the high-throughput screening of MOFs (see Sec. V A below). Jensen et al. simulated the transition dipole moments and the photoluminescence spectra for a Zn-based MOF, RPM3-Zn, in the presence of nitroaromatic guests.[94] Computed photoluminescence quenching was in a good agreement with the experimentally measured one and is attributed to the shift of the lowest unoccupied molecular orbital from the framework to the guest. This selective photoluminescence
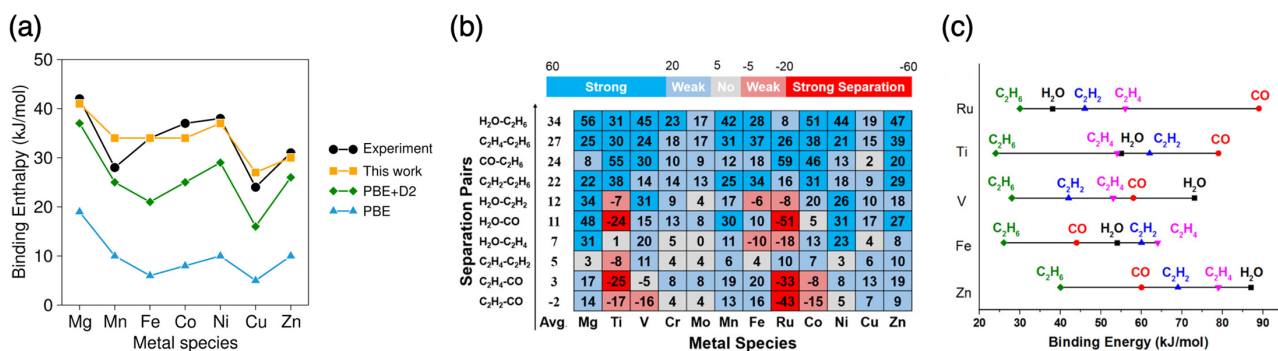
FIG. 3. (a) CO_2 binding enthalpies in M-MOF-74 at 297 K, measured experimentally and computed using PBE, PBE-D2, and vdW-D2 + U2 (with the inclusion of vibrational effects; labeled "this work") levels of theory. Reproduced with permission from Lee et al., Chem. Mater. **27**, 668 (2015). Copyright 2015 American Chemical Society.[77] (b) Average PBE-D3 binding energy differences of 10 pairs of molecules for isostructural M-BTC MOFs with 12 metal centers. Molecular pairs are ordered vertically in the order of decreasing energy difference averaged over all materials. (c) Five types of orderings of computed guest molecule binding energies in M-BTC MOFs. Co and Mg (not shown) have the same ordering as V; Cr, Mo, Mn, Ni, and Cu (not shown) have the same ordering as Zn. Reproduced with permission from You et al., J. Phys. Chem. C **122**, 27486 (2018). Copyright 2018 American Chemical Society.[83]

quenching by nitroaromatics potentially enables the sensing of explosives by the studied MOF.

Periodic computations for MOF–guest systems generally focus on gaseous guests. On one hand, this is because applications involving gases, such as hydrogen storage or flue gas separation, are among the most common ones. On the other hand, this can be attributed to the difficulty of obtaining good starting geometries for large guests in MOFs. Starting structures can be based on chemical intuition,[95] electrostatic complementarity,[80] or modeling using force fields.[84,96,97] Although the choice of a starting geometry is crucial for correctly predicting the final adsorption site, it is often overlooked in the literature.[94,98,99] Devautour-Vinot et al.[96] examined the adsorption of caffeine on functionalized UiO-66(Zr) MOFs with periodic DFT computations. This MOF has tetrahedral and octahedral cages. The authors found that all starting configurations in the tetrahedral cage converge to the same geometry and that this adsorption site is preferred over the ones in the octahedral cage. Despite these difficulties, there are many reasons why periodic computations are important for large guests. The more space the guest occupies in the pore, the more sites are available for its interactions with the host. To describe all these interactions properly, either very large finite models or periodic computations are required. Moreover, the steric hindrance within the framework can only be captured in the periodic setting. Finally, and importantly, periodic computations are necessary to model the long-range interactions and crystal field effects.
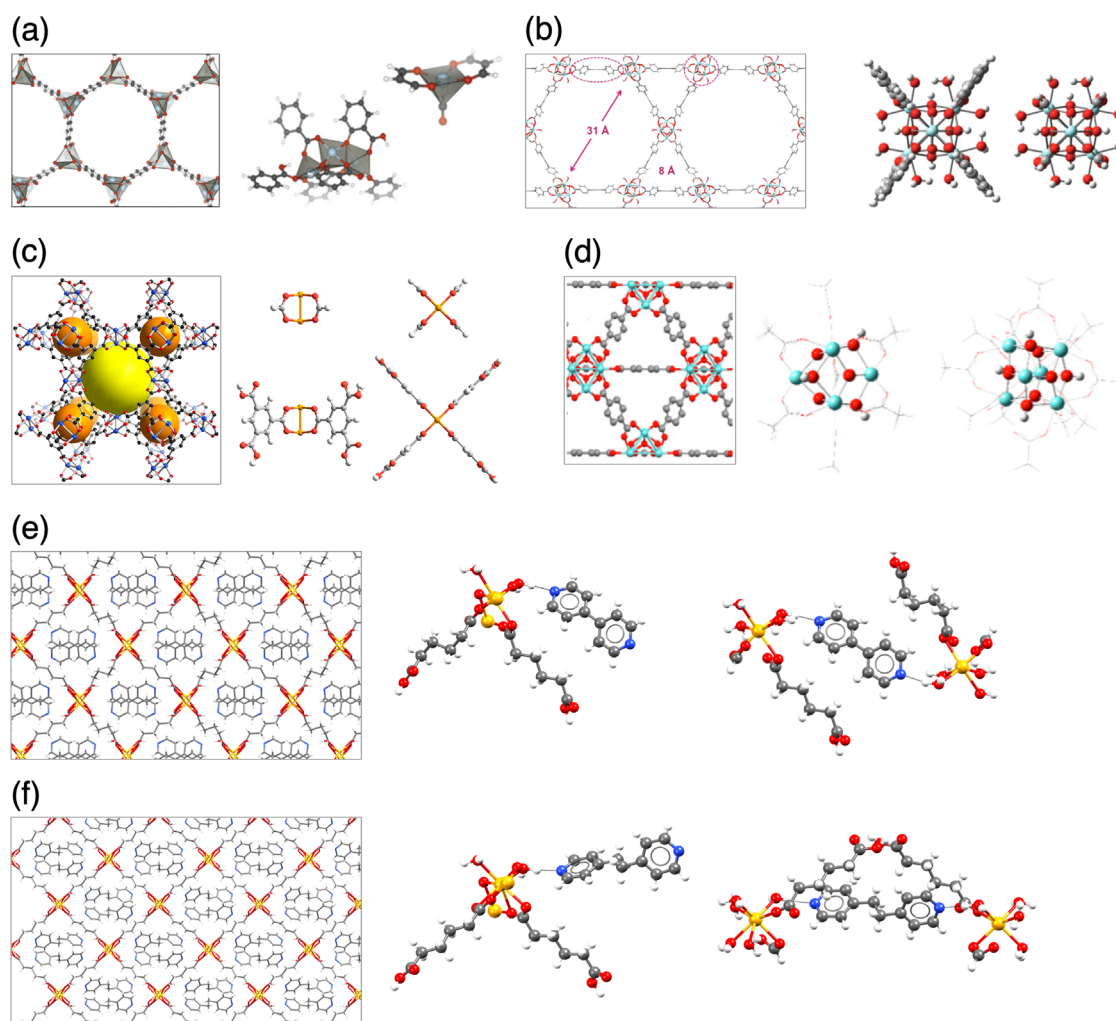
B. Finite models

While periodic models adequately reflect the realistic structure of the framework material, their sheer size prohibits the use of advanced *ab initio* methods, capable of accurately describing static and dynamic electron correlation, which can be critical in multireference (e.g., containing open-shell metal sites) and weakly bound systems (such as many host–guest complexes). To capture these effects, density functionals beyond GGA, as well as single- and multireference post-HF methods can be employed provided the studied system is small enough to make such computations feasible.[100] This is achieved by "cutting out" smaller, finite clusters out of the periodic structures (experimental or optimized *in silico*) of the guest-occluded frameworks, and "saturating" them with, e.g., hydrogen atoms to preserve charge. The cluster is typically defined based on chemical intuition and includes the metal center (in the case of MOFs), the guest molecules, and the parts of the framework interacting with or closest to it (Fig. 4); to the best of our knowledge, this process is yet to be automatized. Numerous methods and codes are available to analyze the energy, electron density, and orbitals in the finite setting. For example, the latter, straightforwardly obtained with finite computations, must instead be constructed from projections in the periodic case.

Many common exchange-correlation density functionals lack in their treatment of dynamic correlation, which is the key component of the attractive interactions between small gas molecules and organic frameworks. To overcome this limitation, in their studies of N_2/CH_4 separation in V-MOF-74 and Fe-MOF-74, Lee et al. employed a non-local Rutgers-Chalmers van der Waals density functional with the Hubbard U correction (vdW-DF2+U), several Minnesota density functionals containing the kinetic energy density term (M06-L, M06, and M11-L), and two wavefunction theory methods: local-pair natural-orbital coupled cluster theory with single and double excitations

(LPNO-CCSD), and complete active space second-order perturbation theory with counterpoise corrections (CASPT2-CP).[101] DFT computations were performed on the periodic model and clusters of two sizes: a "large" cluster containing 88 atoms, including three metal centers, and a "small" cluster composed of 19 atoms, including one metal center [Fig. 4(a)]; the wavefunction theory methods were only feasible for the finite models. Across all models and methods there is a good agreement in terms of the adsorption preference for H_2 vs CH_4 on the two studied MOFs: Fe-MOF-74 does not display any appreciable selectivity, while for V-MOF-74, N_2 binds much stronger than CH_4 (Table I). Similarly, Supronowicz et al. observed an excellent agreement (less than $2 \, kJ \, mol^{-1}$ difference) between B3LYP-D3/TZVP and CCSD(T)/CBS interaction energies of H_2O with a $Cu_2(HCOO)_4$ finite model of the HKUST-1 MOF.[102] They also showed that increasing the basis set size from TZVP to def2-QZVPP does not change the qualitative trends in the binding energies of various gases on the finite model of HKUST-1, and leads to only minor decrease in their absolute values. Koukaras et al. also showed that PBE/def2-TZVPP interaction energies of amino acids (glycine and tyrosine) in IRMOF-14 are in good agreement with the MP2 results.[103]

Multiconfigurational wavefunction methods become indispensable when an accurate description of the open metal sites is required. Stoneburner et al. investigated interaction energies between various gases and M-catecholate MOFs for M = Mg^{2+}, Sc^{2+}, Ti^{2+}, V^{2+}, Cr^{2+}, Mn^{2+}, Fe^{2+}, Co^{2+}, Ni^{2+}, Cu^{2+}, and Zn^{2+} using complete and restricted active space (CAS and RAS, respectively) formalisms of the self-consistent field and second-order perturbation theory (SCF and PT2, respectively), in addition to various flavors of DFT.[104,105] Again, a good agreement was achieved for the overall trends across all tested methods [Fig. 5(a)]. Importantly, multireference methods not only provide more accurate energetics compared to the DFT but also yield physical insight into the host–guest interactions. Bernales et al. turned to multiconfigurational methods in conjunction with the DFT geometries to study the catalytic mechanism of ethylene dimerization by a cobalt(II) or a nickel(II) single-site catalyst supported on the zirconia-like nodes of the NU-1000 MOF [Fig. 4(b)].[106] Analysis of the complete active space molecular orbitals in the rate-limiting transition state allowed explaining superior catalytic activity of the Ni(II) active site compared to Cu.

Depending on the studied system and its application, the size of the cluster model must be adjusted. For example, a cluster consisting of only the linker was sufficient to investigate the influence of OH linker functionalization on the drug delivery performance of IRMOF-16.[107] Pirillo and Hijikata studied how the adsorption properties of several gases at the open metal site of a rhodium paddle-wheel unit are influenced by guests adsorbed on the unit's other side.[108] To consider this effect across a metal–metal bond, a cluster model containing only the metal node was sufficient. Most cluster models consist of one metal node and one or several linkers, which allows capturing (to a certain extent) the interplay between these structural units.[109] However, when multiple adsorption sites in a pore are likely important, the model must contain a large portion of, or even an entire pore. For instance, Supronowicz et al. used a model of an entire pore of HKUST-1 to study the interaction of various biologically important organic molecules with this MOF containing undercoordinated copper centers.[110] Ernst and Gryn'ova probed the importance of the appropriate cluster model choice for the adsorption of 4,4′-bipyridine and 1,2-bis(4-pyridyl)ethane on GW-MOF.[111] Considering two model clusters for each

FIG. 4. Periodic guest-free and guest-occluded metal–organic frameworks (gray border) and their corresponding finite (cluster) models (no border). (a) Periodic and two cluster models of V-MOF-74 (element colors: light blue—vanadium, red—oxygen, dark gray—carbon, and white—hydrogen atoms). Adapted with permission from Lee *et al.*, J. Am. Chem. Soc. **136**, 698 (2014). Copyright 2014 American Chemical Society.[101] (b) Zr6-based framework of NU-1000 and the corresponding benzoate and formate cluster models (element colors: gray—carbon, white—hydrogen, cyan—zirconium, red—oxygen). Adapted with permission from Bernales *et al.*, J. Phys. Chem. C **120**, 23576 (2016). Copyright 2016 American Chemical Society.[108] (c) HKUST-1 MOF and its molecular cluster models, dicopper tetraformate Cu₂(HCOO)₄ (top) and dicopper tetrabenzenetricarboxylate Cu₂BTC₄ (bottom), side (left) and top (right) views (element colors: orange—copper, gray—carbon, red—oxygen, white—hydrogen). Adapted with permission from Supronowicz *et al.*, J. Phys. Chem. C **117**, 14570 (2013). Copyright 2013 American Chemical Society.[102] (d) UiO-66 MOF and its model cluster representing the Zr6 node from two views (element colors: gray—carbon, white—hydrogen, cyan—zirconium, red—oxygen). Adapted with permission from Yang *et al.*, J. Am. Chem. Soc. **137**, 7391 (2015). Copyright 2015 American Chemical Society.[113] (e) and (f) Crystal packing of GW-MOF occluded with 4,4'-bipyridine (e) and 1,2-bis(4-pyridyl)ethane (f) guests, view in *c* direction, as well as two cluster models for each complex (element colors: white—hydrogen, gray—carbon, blue—nitrogen, red—oxygen, and yellow—calcium). Adapted with permission from M. Ernst and G. Gryn'ova, ChemPhysChem **23**, e202200098 (2022). Copyright 2022 Authors, licensed under a Creative Commons Attribution-NonCommercial-NoDerivatives (CC BY NC ND) license.[111]

guest, adsorption energies were computed for both the periodic and the finite models [Figs. 4(e) and 4(f)] at a range of DFT levels; these were subsequently refined and analyzed using energy decomposition analyses (EDAs)[112] to identify the physical underpinnings of the host–guest interactions (see Sec. III D below). Larger clusters including two metal centers closely reproduced the trends in the interaction energy from the periodic model, while predictions for the smaller clusters led to qualitatively wrong trends [Fig. 5(b)].

Cluster models are often employed to investigate the mechanisms of reactions inside the framework materials using density functionals beyond the generalized-gradient approximation, common in the periodic approaches. For example, the M06-L functional, which includes short-to-medium-range van der Waals interactions, has been successfully applied to study mechanisms of catalytic ethylene hydrogenation and dimerization by Ir(CO)₂ and Ir(C₂H₄)₂ complexes on UiO-66 and NU-1000 supports [Fig. 4(d)],[113] catalytic propane oxidative

TABLE I. N_2/CH_4 adsorption energy differences for M-MOF-74 (in kcal mol^{-1}), computed using periodic and two cluster models. Reproduced with permission from Lee *et al.*, J. Am. Chem. Soc. **136**, 698 (2014). Copyright 2014 American Chemical Society.[101]

Level of theory	V	Fe	V	Fe
			Periodic	
			6.0	0.4
vdW-DF2+U	Small		Large	
vdW-DF2+U	4.9	0.4	5.8	0.3
M06-L	4.3	0.0	10.1	0.9
M06	4.5	0.1	6.9	0.4
M11-L	4.2	−0.8	5.9	−1.7
LPNO-CCSD/CBS	4.8	0.7	. . .[a]	. . .[a]
CASPT2 CP	3.8	0.3	2.1	0.3

[a]Impractically computationally intensive.

dehydrogenation by activated Co-SIM+NU-1000 MOF,[114] and carbonyl-ene reaction between encapsulated formaldehyde and propylene on M3(btc)$_2$ (M = Fe, Co, Ni, Cu and Zn).[115] Chen *et al.* used B3LYP to investigate the catalytic hydrolysis of organophosphate warfare agents by MOF NU-1000 after benchmarking HF, M06, M06–2X, B3LYP, and a modified complete basis set method (CBS-QB3) on the uncatalyzed reaction.[116] Islamoglu *et al.* used the M06-L functional to study the effect of amino groups in proximity of metal nodes on the organophosphate decomposition reaction.[117]

Complete-active space approaches, CASSCF and CASPT2, can be employed to refine the DFT energies in multireference systems, as was done in the study of CH-activation mechanism by MIL (Materials of Institute Lavoisier) metal–organic frameworks.[118] Such

multiconfigurational approaches become indispensable when modeling optically active systems, such as MOF-based luminescent sensors for small molecules. Hidalgo-Rosa *et al.* investigated the luminescence quenching in a Eu-MOF sensor for aniline[119] and a Cd-MOF sensor for 4-nitroaniline[120] at a cluster model level using CASSCF and NEVPT2 methods in addition to time-dependent density functional theory, elucidating the energy transfer pathways crucial for the turn-off luminescence mechanism of these chemosensors (Fig. 6). To investigate the hydrogen bond between formaldehyde and the luminescent MOF [Zn(NH$_2$bdc)(bix)]$_n$, Yao *et al.* also used time-dependent density functional theory (CAM-B3LYP functional) and established that luminescence is due to the ligand-to-ligand rather than ligand-to-metal charge transfer.[121]

C. Hybrid models

Instead of choosing between the periodic and finite models, combining them can yield an in-depth insight into the electronic structure whilst preserving a realistic representation of the system. Such "hybrid" approaches often employ periodic computations at the LDA and GGA level with subsequent geometry and energy refinement on a cluster model at higher-rung DFT and post-HF levels of theory. Dixit *et al.* demonstrated that periodic PBE computations adequately describe the hydrogen adsorption on MOF-5 (M = Li, Be, Mg, and Al) when compared to hybrid DFT and MP2 cluster modeling.[122] A hybrid approach coined MP2:B3LYP+D* was introduced to quantify the interaction of CO and CO$_2$ with the CPO-27-M metal–organic frameworks (M = Mg^{2+}, Ni^{2+}, Zn^{2+}): the structures of adsorption complexes were generated at the B3LYP-D* level with periodic boundary conditions, and their interaction energies were computed for representative clusters using perturbation theory.[123] This approach reproduces the experimental sequence of binding energies for the metal centers, and yields heats of adsorption within *ca.* 2 kJ mol^{-1} of the experimental values. Similarly, a hybrid MP2:(PBE+D2)
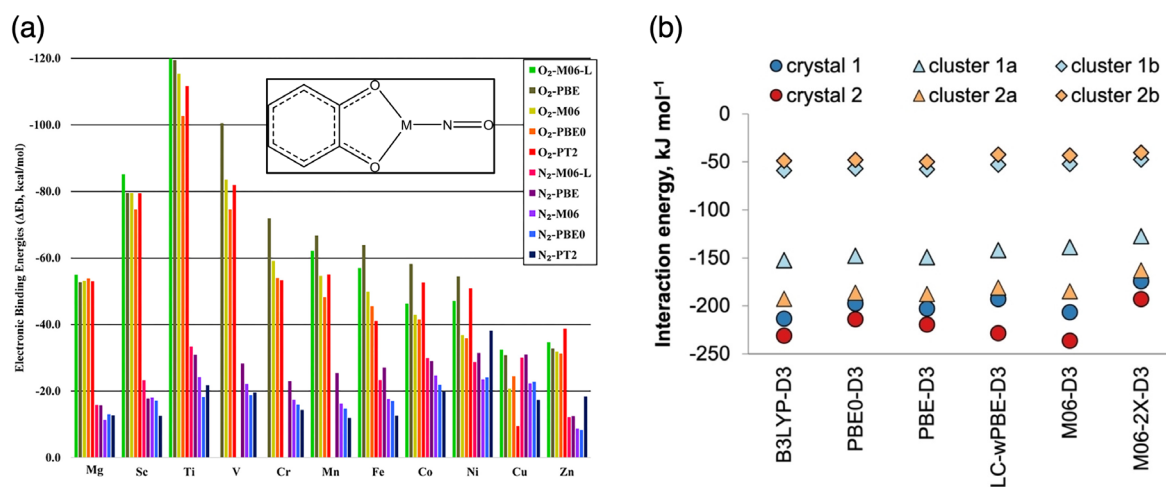
FIG. 5. (a) Computed DFT and PT2 electronic binding energies (in kcal mol^{-1}) of O$_2$ and N$_2$ to cat–M^{2+} systems. M06-L results are absent for Mn–N$_2$, V, and Cr because of convergence failures. Inset: structure of NO bound to the cat–M complex. Adapted with permission from S. J. Stoneburner and L. Gagliardi, J. Phys. Chem. C **122**, 22345 (2018). Copyright 2018 American Chemical Society.[104] (b) Host–guest interaction energies in periodic (per guest molecule, i.e., ΔE/4, as there are four guest molecules per unit cell) and cluster models of the studied systems, computed using a range of density functionals. Reproduced with permission from M. Ernst and G. Gryn'ova, ChemPhysChem **23**, e202200098 (2022). Copyright 2022 Authors, licensed under a Creative Commons Attribution-NonCommercial-NoDerivatives (CC BY NC ND) license.[111]
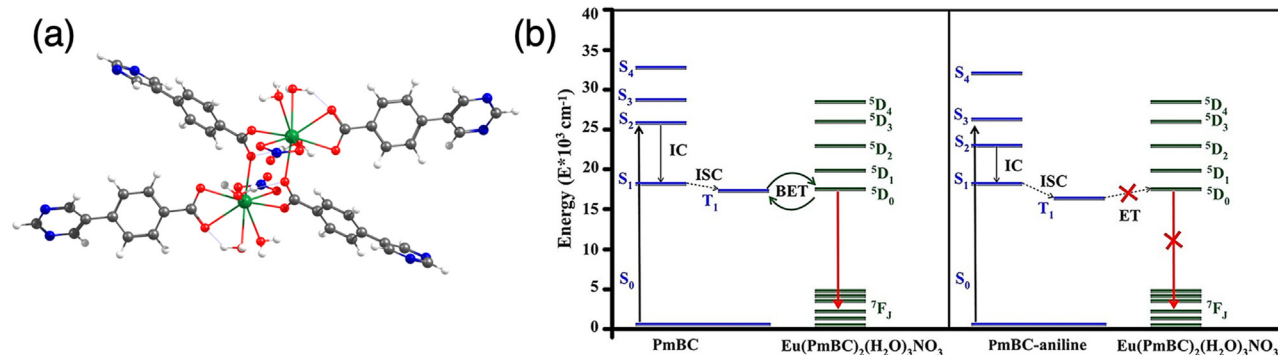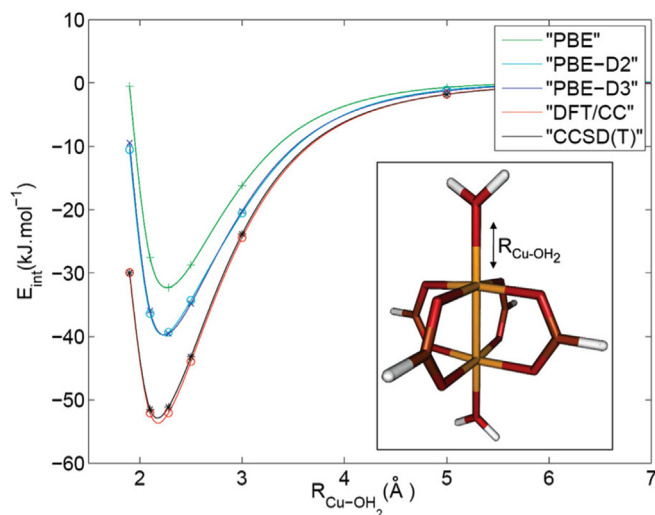
FIG. 6. (a) Structural model of the dimer building unit [Eu$_2$(PmBC)$_4$(NO$_3$)$_2$H$_2$O)$_6$] (labeled here "Eu-MOF") of the EuL MOF consisting of Eu^{3+} metal centers and 4-(pyrimidin-5-yl) benzoate (PmBC) linkers. (b) Energy transfer pathway for the sensitization and emission of the Eu-MOF system. All states were determined at the CASSCF/NEVPT2 level of theory with an active space of CAS(8,8) for the PmBC, CAS(8,8) for the PmBC-aniline, and CAS(6,7) for the europium fragment. IC—internal conversion, ISC—intersystem crossing, ET—energy transfer, and BET—back energy transfer. Reproduced with permission from Hidalgo-Rosa et al., J. Comput. Chem. **41**, 1956 (2020). Copyright 2020 Wiley-VCH GmbH.[119]

+ΔCCSD(T) method, in which PBE-D2 is used to optimize the adsorption complexes and compute their anharmonic frequencies, and the accurate electronic energies of cluster models are computed at the MP2 level with a correction for higher-order correlation effects at the CCSD(T) level, was used to estimate the adsorption energies of CO on CPO-27-Mg.[124] The computed adsorption isotherms are in close agreement with experiment, with only ~1 kJ mol^{-1} deviation in Gibbs free energies. Nachtigall and co-workers introduced a so-called DFT/CC approach, in which a correction term, computed for a cluster model using DFT, CCSD(T) and ΔMP2 extrapolation to complete basis set limit, is added to the periodic PBE/PAW results to approximate the CCSD(T)/CBS accuracy (Fig. 7).[125,126] When applied to

model CO$_2$ adsorption on CuBTC MOF, this method yields a very good agreement with experiment.[127] Finally, Yu et al. developed an MP2-based QM/MM method to compute the binding energy of CO$_2$ on CPO-27-M (M = Mg, Mn, Fe, Co, Ni, Cu, and Zn).[128] As in the previous examples, the adsorption complex geometries were first relaxed using periodic DFT (PW91 functional), and subsequently used to cut out finite clusters. Geometries of these clusters were further refined at the B3LYP/6-31+G(d,p) level, and their energies computed at the MP2/6-31+G(d,p) level of theory. These finite-model ab initio adsorption energies were then corrected to account for the periodicity of the real system using molecular mechanics (Dreiding and Universal force fields). This approach afforded good agreement with experimental heats of adsorption (Table II).

D. In-depth analysis of the host–guest interactions

A good tactic in football involves understanding the interaction between the players and the ball in detail. Likewise, a good tactic for designing MOFs and COFs requires detailed insight into the host–guest interaction mechanism and type. Diverse approaches to analyzing the non-covalent interactions are well established for molecular chemistry and reactivity,[129,130] biomolecular complexes,[131,132] molecular crystals,[133,134] but are somewhat less common in MOF-guest systems. Among these approaches, energy decomposition techniques discern the energetic contributions to the total interaction energy and the physical forces behind the interactions, while analysis of canonical and/or localized orbitals, as well as electron density and its derivatives allow localizing, quantifying, and visualizing the interactions.

Energy decomposition analyses (EDAs) yield quantitative partitioning of the interaction energy into physically meaningful components, e.g., electrostatic, Pauli repulsion, polarization, orbital mixing, and dispersion term. Tsivion et al. used absolutely localized molecular orbital energy decomposition analysis (ALMO-EDA) to study the interaction of hydrogen molecules with typical MOF linkers.[135] While interactions with the non-metalated linkers are driven by dispersion and weak charge transfer, they range from significant charge transfer to mostly electrostatic in metalated linkers depending on their polarity. Similarly, the ethylene dimerization by fluorinated organic

FIG. 7. The interaction energy of H$_2$O with the Cu$_2$(HCOO)$_4$ cluster model (depicted in the inset) as a function of the R$_{Cu-OH_2}$ distance computed at different levels of theory (element colors: yellow—copper, red—oxygen, orange—carbon, and white—hydrogen). Reproduced with permission from Grajciar et al., J. Phys. Chem. Lett. **1**, 3354 (2010). Copyright 2010 American Chemical Society.[126]

TABLE II. Computed CO_2 binding energies (in kJ mol^{-1}) and experimental heats of adsorption Q_{st} (in kJ mol^{-1}). Reproduced with permission from Yu *et al.*, Chem. Sci. **4**, 3544 (2013). Copyright 2013 Royal Society of Chemistry.[128]

MOF	LDA periodic	GGA periodic	LSDA cluster	B3LYP cluster	MP2 cluster	QM/MM periodic	Q_{st}[a]
Mg	−54.3	−23.9	−63.0	−23.9	−40.5	−48.2	42.0, 47, 39, 73, 42
Mn	−38.4	−13.3	−43.2	−12.1	−30.3	−37.2	31.9
Fe	−38.1	−9.4	−36.6	−4.48	−24.2	−32.2	34.3
Co	−42.5	−10.6	−43.2	−7.70	−29.7	−37.0	34.5, 37
Ni	−43.1	−12.5	−52.9	−11.2	−31.2	−39.1	38.7, 41
Cu	−31.0	−6.0	−27.4	−3.49	−16.2	−23.9	24
Zn	−40.2	−12.4	−50.4	−11.8	−29.7	−37.0	30.6

[a]By convention, the isosteric heat of adsorption is a positive quantity; please see Ref. 112 for the sources of the experimental data.

ligand on palladium MOF catalysts[109] and the H_2 adsorption on a vanadium MOF[136] were analyzed with the ALMO-EDA approach. The Kitaura–Morokuma-Ziegler EDA was used to explain the selective adsorption of certain gas molecules on rhodium and copper paddle wheel nodes,[108] and to examine the interactions of H_2, CH_4, C_2H_4, C_2H_6, CO_2, and CS_2 with a Hofmann-type MOF, modeled by a gas molecule sandwiched between two pyrazine molecules.[137] Furthermore, the Morokuma–Ziegler EDA, the natural orbitals for chemical valence (NOCV) approach, and the non-covalent interactions index (NCI) were employed to investigate the charge transfer channels between MOF $[Zn_2(OBA)_4(BYP)_2]$ and nitrobenzene, and between MOF $[Cd_2(H_2L)_2(H2O)_5]_{0.5}H_2O$ explaining the turn-off mechanism of luminescence in these chemosensing MOFs.[120,138] Symmetry-adapted perturbation theory (SAPT) revealed dispersion and electrostatics as main forces behind the sorption of H_2 on the open metal sites of HKUST1-MOF, while dispersion and induction were found to be the main contributors to the selective adsorption of krypton over xenon in an ultramicroporous MOF $[Ca(C_4O_4)(H_2O)]$ [Fig. 8(a)].[139,140]

Koukaras *et al.* investigated IRMOF-14 and IRMOF-16 for the delivery of an anticancer agent tamoxifen.[141] Organic linkers of the two MOFs were modified by inserting a hydroxyl group to enable hydrogen bonding with tamoxifen. Based on the spin-component scaled second-order Møller–Plesset perturbation theory [SCS(MI)-MP2] computations, OH-IRMOF-16 has a higher binding affinity toward tamoxifen than OH-IRMOF-14. To further analyze the interactions responsible for this preference, the non-covalent interaction index method was applied to the cluster model of hydroxy-functionalized IRMOF-16. NCI confirmed the strong attractive hydrogen bonding interaction between the nitrogen atom of tamoxifen and the hydroxyl unit of the MOF linker [Fig. 8(b)]. Tan *et al.* used DFT and NCI to explain the experimentally observed high adsorption selectivity for methanol and ethanol over other volatile organic compounds on DPPB-2 (the amorphized form of MOF DPPB-1).[142]

Ernst and Gryn'ova compared SAPT and Bickelhaupt–Baerends EDAs, as well the NCI and density overlap regions indicator (DORI) tools for two types of cluster models of the GW-MOF hosting 4,4'-bipyridine or 1,2-bis(4-pyridyl)ethane. Both EDA methods yielded the same qualitative results (Fig.9), whilst both NCI and DORI confirmed that the host–guest interactions are dominated by hydrogen bonds.[111]

IV. TEAM PLAY: THE MACROSCOPIC PROPERTIES

So far, this review focused on the host–guest interactions in the context of capture/adsorption, storage, transformation, and release of the guests. However, guests can also affect the macroscopic bulk properties of the MOFs. A prominent example is the breathing effect of certain MOFs possessing a dynamic framework. In their pioneering work, Loiseau *et al.* investigated the structural basis for the large breathing effect observed for MIL-53 upon hydration. The water
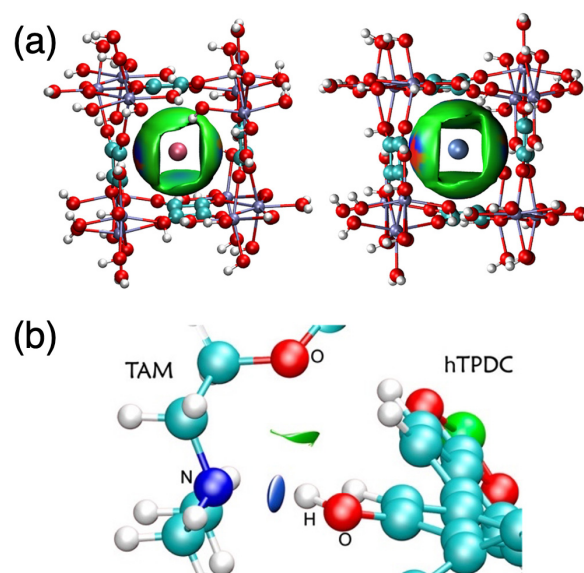
FIG. 8. (a). Intermolecular interactions (0.00155 a.u. isovalue) in Kr@UTSA-280 (left) and Xe@UTSA-280 (right), visualized using the independent gradient model analysis. In these isosurfaces, blue represents a strong attraction, green—van der Waals interaction, and red—strong repulsion over the electron density range of $-0.05 < \rho(r) < 0.05$ a.u. Reproduced with permission from Xiong *et al.*, J. Phys. Chem. C **124**, 14603 (2020). Copyright 2020 American Chemical Society.[140] (b) Partial view of the structures of tamoxifen (TAM, left) and the hTPDC organic linker (right), and the reduced density gradient isosurface ($s = 0.5$ a.u.) for the region between the N_{TAM} and the HO_{hTPDC}. The blue color of the surface corresponds to a negative $\sin(\lambda_2)\rho$ and indicates a strong and attractive noncovalent, acid–base interaction. Reproduced with permission from Koukaras *et al.*, J. Phys. Chem. C **118**, 8885 (2014). Copyright 2014 American Chemical Society.[141]
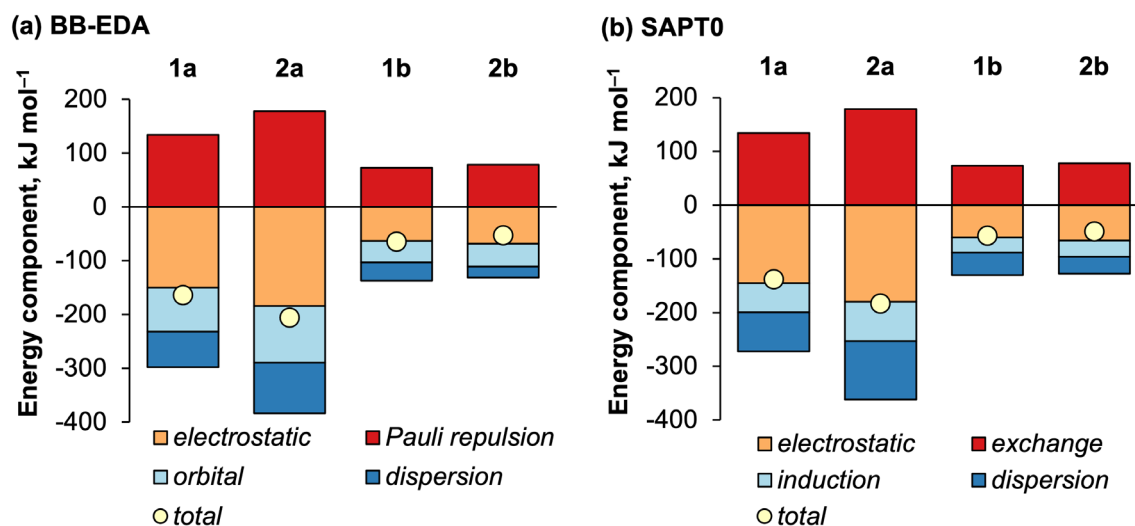
FIG. 9. Energy decomposition analyses in two cluster models, (a) and (b), of GW-MOF complexes with 4,4′-bipyridine and 1,2-bis(4-pyridyl)ethane. Reproduced with permission from M. Ernst and G. Gryn'ova, ChemPhysChem **23**, e202200098 (2022).Copyright 2022 Authors, licensed under a Creative Commons Attribution-NonCommercial-NoDerivatives (CC BY NC ND) license.[111]

molecules in the one-dimensional channels of this highly flexible MOF form hydrogen bonds with the framework, causing a substantial change in the pore size whilst preserving the topology.[143] The breathing effect influences not only the pore size but also the magnetic[144] and mechanical[145] properties of MOFs.

Dong *et al.* evaluated the elastic tensors of MOF-901 free of solvent and occluded with 5.7 and 11.4 wt. % methanol. According to DFT (PBE) computations of the unit-cell compression, the stability of MOF-901 increases with increasing methanol content, likely due to methanol molecules filling the pores and leading to greater structural stability.[146] Canepa *et al.* computed the elastic constants, bulk, shear, and Young's moduli of empty MOF-74-Zn and loaded with H_2, CO_2, CH_4, and H_2O using the vdW-DF functional.[147] The incorporation of the adsorbates generally leads to a substantial increase in the elastic constants, indicative of the loss in the MOF's flexibility. The largest increase is induced by water, which was also found to have the strongest interaction with the framework. Furthermore, the adsorbate-induced changes to the MOF's heat capacity, computed from the *ab initio* phonon frequencies, were found to be related to the host–guest interaction energy: the larger the energy, the larger the heat capacity [Fig. 10(a)]. Specifically, the largest heat capacity among the studied guests were found for water, in line with the interaction energies: $-73.9\,kJ\,mol^{-1}$ for H_2O, $-52.4\,kJ\,mol^{-1}$ for CO_2, $-40.1\,kJ\,mol^{-1}$ for CH_4, and only $-20.9\,kJ\,mol^{-1}$ for H_2.

Water molecules in the pores also affect the electric properties of MOFs. Using a combination of periodic DFT computations, impedance measurements, accurate X-ray diffraction measurements and charge density modelling, Scatena *et al.* showed that the dielectric constant of HKUST-1 differs substantially depending on whether its pores are empty, half-filled, or filled with water molecules [Fig. 10(b)].[148] For the same MOF, it was shown that introducing 7,7,8,8-tetracyanoquinododimethane (TCNQ) guest molecules leads to a six orders of magnitude increase in the electrical conductivity.[149] *Ab initio* calculations suggest that every TCNQ guest molecule bridges four copper paddle

wheel units. This guest molecule introduces an additional empty band into the band gap of the MOF, resulting in a new charge transfer band. Similarly, guests have been shown to affect the framework's magnetic properties. For example, periodic vdW-DFT computations were employed to investigate the spin-crossover transition temperature in empty and guest-occluded {Fe(pyrazine)[Pt(CN)$_4$]} MOF.[150] Crystal orbital displacement curves were computed to analyze the stabilization or destabilization due to the host–guest interactions and the charge transfer between the host and the guest.

Luminescent MOFs find potential application in light-emitting diodes, lasers, and as chemical sensors.[99] When used as the latter, their fluorescence (and phosphorescence) is selectively turned on or off by guest molecules based on their type and/or quantity and tuned by the host–guest interactions. Yang and Yan studied the fluorescence of 4-(dicyanomethylene)-2-methyl-6-(4-dimethylaminostyryl)-4H-pyran (DCM) incorporated into stilbene-MOF and IRMOF-8. DCM is a laser dye with red fluorescence, while these MOFs show blue emission under UV irradiation. The incorporation of DCM into them resulted in a blue/red two-color emission. Periodic DFT computations demonstrated that an energy transfer from the MOF to the DCM molecule occurs during the excitation process. Furthermore, the authors probed the luminescence response of the host-guest systems when volatile organic solvents were added. This affected the emission wavelength and the intensity ratio of the blue to red emission, which demonstrates that these MOF-DCM systems could be useful ratiometric luminescence sensors. The phosphorescence of two Zn-terephthalate (TPA) MOFs, 1-DMF and MOF-5, upon treatment with a pyridine solution was also investigated.[151] Frontier orbital analysis revealed that in the empty MOF the HOMO is mainly located on Zn$_2$O$_8$ metal nanoclusters, while the LUMO is primarily located on the TPA ligands. Pyridine guest introduces intermediate energy levels participating in the photoemission process and shifting the wavelength of the emission. Hidalgo-Rosa *et al.* rationalized the selective fluorescence quenching in [Zn$_2$(OBA)$_4$(BPY)$_2$] MOF by nitrobenzene but not by
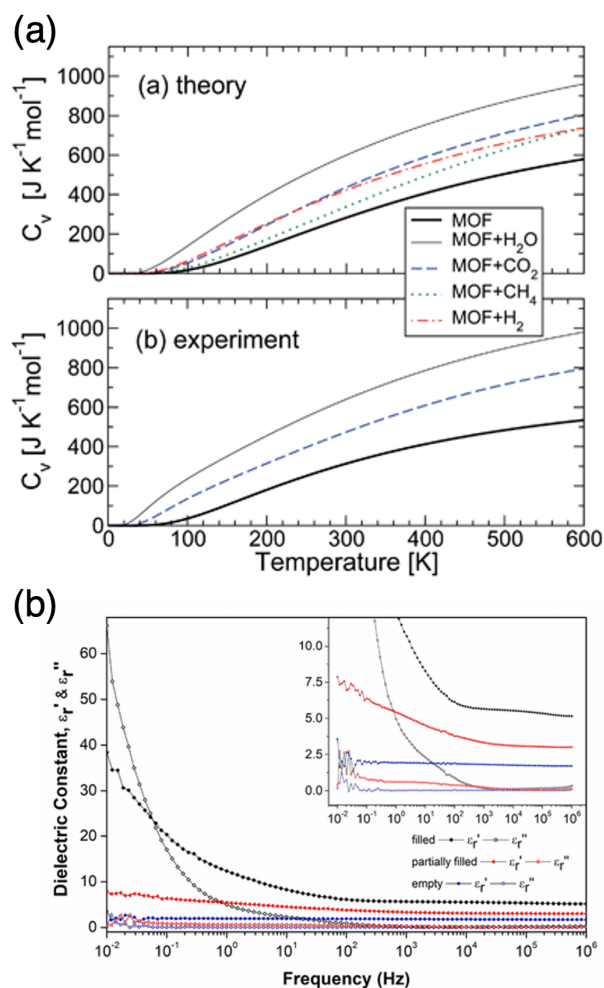
FIG. 10. (a) Constant volume heat capacity, C_ν, for an empty MOF-74-Zn and loaded with H_2, CO_2, CH_4, and H_2O, computed from *ab initio* frequencies omitting phonon frequencies below $500\,cm^{-1}$ (top) and computed from experimental IR frequencies between 500 and $3800\,cm^{-1}$ (only for CO_2 and H_2O, bottom). Reproduced with permission from Canepa *et al.*, J. Mater. Chem. A **3**, 986 (2015). Copyright 2015 Royal Society of Chemistry.[147] (b) Real (ε_r') and imaginary (ε_r'') dielectric constant for HKUST-1 as-synthesized (filled with H_2O and MeOH), measured in air after activation (partially filled with H_2O), and measured in N_2 after activation (empty). The inset highlights the differences between activated samples measured in different atmospheres. Reproduced with permission from Scatena *et al.*, J. Am. Chem. Soc. **141**, 9382 (2019). Copyright 2019 Authors, licensed under an ACS AuthorChoice license.[148]

toluene using time-dependent DFT and finite models.[119] They showed that the fluorescence emission is due to a linker-to-linker charge transfer involving π-type orbitals. DFT geometry optimizations revealed that the absorption of nitrobenzene leads to the formation of host-guest hydrogen bonds. In this system, the LUMO is now located on nitrobenzene, from which the energy dissipates through the nonradiative transition resulting in the turn-off of the fluorescence. Instead, toluene does not introduce a LUMO between the HOMO and LUMO of the empty MOF.

## V. TALENT SCOUTS: INSIGHT FROM ARTIFICIAL INTELLIGENCE

A. High-throughput screening

Given the enormous number of possible metal–organic frameworks, selecting the structure most suited to a specific application (i.e., a specific guest molecule) necessitates efficient and rapid techniques to explore this vast chemical space. High-throughput screening (HTS) approaches benefitting from continuously increasing computer power and improving simulation algorithms enable searching thousands of structures according to target criteria. These approaches typically involve either constructing a new or utilizing an existing database of MOFs, such as the Computation-Ready, Experimental (CoRE) metal–organic framework database,[152] computing their relevant physico-chemical properties (descriptors) using an appropriate, i.e., simultaneously sufficiently accurate and computationally feasible method, and ranking the structures so as to identify the most promising candidates.[153,154]

In 2012, the Snurr research group constructed an extensive database of hypothetical MOFs (ca. 138 000 structures) from the building blocks of existing frameworks;[155] this hMOF database is available at http://hmofs.northwestern.edu. Since then, it has been repeatedly employed to search for MOFs with desirable adsorption properties, and to identify the relevant structure–property relationships. In the seminal publication,[155] the hMOF database was screened for methane-storage capacity. The most promising candidate, NOTT-107, was then synthesized and shown to outperform the best material for CH_4 storage at the time, PCN-14. Improved materials were discovered in the hMOF database for Xe/Kr separation,[156] and for many other applications by identifying the relevant screening criteria. For example, a clear correlation was established between purely structural (e.g., pore size, surface area, and pore volume) and chemical features (such as functional groups) of MOFs and their gas adsorption properties (Fig. 11).[157] To rapidly identify MOFs with superior hydrogen storage capacity, a simple metric—the binding fraction, i.e., the fraction of the unit cell volume within a given distance of the framework—was introduced and shown to reliably reflect the gas storage capacity of the framework.[158] The ratio of Henry's law constants between CO_2 and H_2O was used to identify MOFs with high CO_2 selectivity under high humidity conditions.[159]

The Grand Canonical Monte Carlo method is among the most frequently used simulation techniques in high-throughput workflows due to its relatively low computational cost. GCMC high-throughput screening allows estimating typical adsorbent selection criteria, such as adsorption selectivity, adsorbent performance score (APS), sorbent selection parameter, working capacity, and regenerability of MOFs. Candidate structures are generally ranked according to a combination of these metrics. This approach was used to discover frameworks with high CO_2/CH_4 selectivity and total loading above 0.5 mol kg^{-1} among ca. 3000 existing MOFs,[160] candidates for separating the dibranched hexane isomers from their linear and monobranched counterparts out of 12 351 existing MOFs,[161] and frameworks for CH_4/H_2 separation among almost 55 000 structures from the Cambridge Structural Database.[162] In the latter example, a simple mathematical model was also proposed to predict the CH_4/H_2 selectivity.

Density functional theory computations, either in a periodic or in a finite fashion, can be included at the later stages of a high-throughput screening workflow to refine the predictions from GCMC
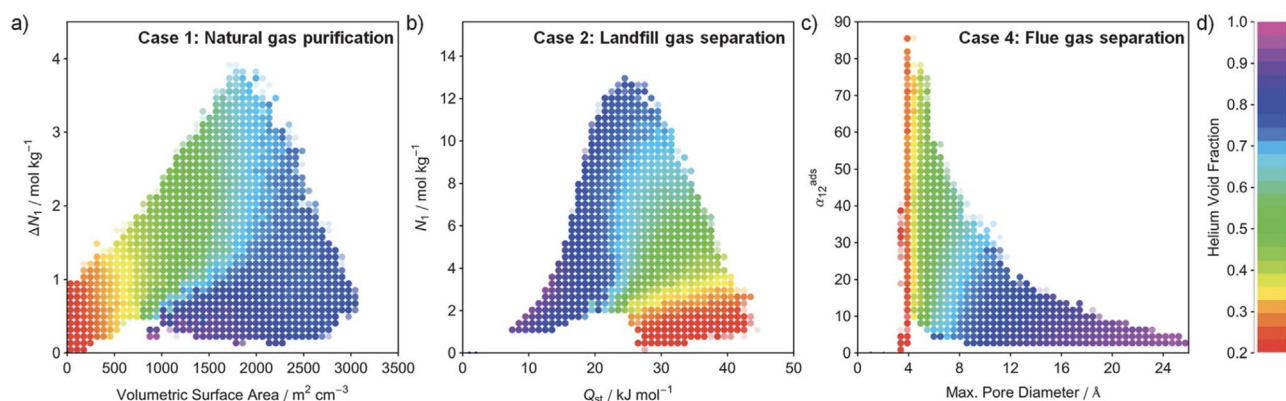
FIG. 11. Exemplary structure–property relationships derived from simulated CO_2, CH_4, and N_2 adsorption in over 130 000 hypothetical MOFs. Clear relationships can be discerned between (a) CO_2 working capacity (ΔN_1) and surface area, (b) CO_2 uptake (N_1) at 2.5 bar and CO_2 heat of adsorption (Q_{st}), and (c) selectivity of CO_2 over N_2 (α_{12}^{ads}) and maximum pore diameter. Q_{st} values are determined from CO_2 adsorption at the lowest simulated pressure (0.01 bar). Each plot is divided into 50×50 regions that are represented by a filled circle if more than 25 structures exist within the region. The color of each circle represents the average (d) helium void fraction of all structures in that plot region. Reproduced with permission from Wilmer et al., Energy Environ. Sci. **5**, 9849 (2012). Copyright 2012 Royal Society of Chemistry.[157]

or other semi-empirical models for selected candidates. Demir et al. screened the CoRE MOFs database for O_2 and N_2 binding using GCMC for the initial selection, and periodic and cluster DFT to compute accurate binding energies.[163] To find the best candidates from the same database for propane/propene separation by diffusion, Pramudya et al. combined molecular dynamics, nudged elastic band (NEB) with the classical UFF-FM force field, and DFT computations in a high-throughput workflow.[164] DFT was particularly necessary when modeling MOFs with long flexible linkers, as the NEB UFF-FM method could not provide reliable energy barrier estimates for these systems. Periodic DFT simulations were also used to obtain accurate geometries of 936 anion-pillared MOFs prior to GCMC simulations of Xe and Kr adsorption in the high-throughput screening of MOFs for Xe/Kr separation.[165]

The entire screening procedure can be performed at the ab initio level instead of classical simulations, typically using the LDA or GGA density functionals. For example, Canepa et al. investigated the adsorption of H_2, CO_2, CH_4, and H_2O in MOF-74-M (M = Be, Mg, Al, Ca, Sc, Ti, V, Cr, Mn, Fe, Co, Ni, Cu, Zn, Sr, Zr, Nb, Ru, Rh, Pd, La, W, Os, Ir, and Pt) using periodic vdW-DF computations, and discovered that only a few noble metals afford selective adsorption of CO_2 over H_2O [Fig. 12(a)].[93] Rosen et al. developed a fully automated, high-throughput periodic density functional theory workflow and applied it to screen the CoRE database for MOF catalysts for methane activation.[166] Periodic PBE-D3(BJ) computations revealed that the oxidation of the open metal site, and not the C–H bond activation in CH_4, is the rate determining step, suggesting that improved MOF heterogeneous catalysts can be achieved with low-valence, redox-active open metal sites. Extending this work, the authors screened 60 MOFs for the catalytic activation of methane and demonstrated that the active site formation energy is a reliable descriptor of both the thermodynamic stability of the metal-oxo active site and the framework's ability to activate the C–H bonds [Fig. 12(b)].[167] Furthermore, Rosen et al. screened a series of MOFs comprised of 6 MOF families (MOF-74, MOF-74-S, MIL-88B, MIL-88B-OH, and MAF-X, where MAF = metal-azolate framework, X = bridging anion, e.g., μ-Br–, μ-

Cl–, μ-F–, μ-SH–, or μ-OH–) and diverse metals (V^{2+}, Cr^{2+}, Mn^{2+}, Fe^{2+}, Co^{2+}, Ni^{2+}, Cu^{2+}, and Zn^{2+} cations for MOFs with M^{2+} binding sites, and Sc^{3+}, Ti^{3+}, V^{3+}, Cr^{3+}, Mn^{3+}, Fe^{3+}, Co^{3+}, and Ni^{3+} cations for MOFs with M^{3+} binding sites) for O_2 and N_2 adsorption.[168] The MOF unit cell shapes and volumes were optimized at the periodic PBE-(D3)BJ level of theory with Hubbard U correction, and the atomic positions and adsorption energies were obtained at the M06-L level. Gas molecules were systematically placed inside the pores using the MOF adsorbate initializer program,[166] and the adsorption modes were analyzed using the CrystalNN bonding topology algorithm.[169] This study elucidated the effect of the bridging anion on the gas adsorption strength and demonstrated how this effect can be utilized to develop more selective MOF adsorbents. Finally, Fumanal et al. based their high-throughput screening of MOF photocatalysts on two energy-based descriptors: the UV-vis light absorption capability and the band energy alignment.[170] Both descriptors were derived from the electronic structure features (bandgap, ionization potential, etc.) assessed at the periodic PBE and (selectively) PBE0 levels of theory.

Apart from physical and chemical descriptors, the topology of the framework itself can be used in the high-throughput screening, as was demonstrated by First et al. for the separation of gases (O_2/N_2, CO_2/N_2, CO_2/CH_4, and CO_2/H_2) and chemicals (propane/propylene, ethane/ethylene, styrene/ethylbenzene, and xylenes) in MOFs.[171] 1690 frameworks were assessed based on the shape selectivity criterion, which considers the minimum-energy pathway of a guest molecule through the material and is evaluated using the MOFomics code.[172]

High-throughput screening generates extensive sets of structural and computed data; thus, tailored approaches are needed to analyze it, to discover promising candidates, and to arrive at practical material design guidelines. Moghadam et al. developed an interactive visualization tool, which assists in analyzing the multidimensional structure–property plots, obtained in the HTS, and identifying the relationships between structural properties and adsorbent performance.[173] Applying this technique in combination with the GCMC and DFT computations to a database of 2932 existing MOFs, the authors identified UMCM-152 MOF as a promising candidate for O_2 storage (Fig.
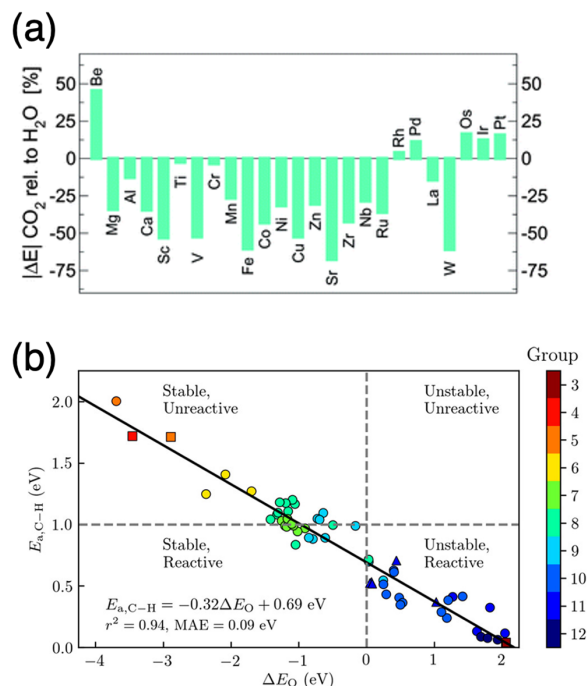
FIG. 12. (a) Magnitude of the adsorption energy of CO_2 relative to H_2O in MOF-74-M. Positive values correspond to CO_2 binding more strongly than H_2O. Reproduced with permission from J. Mater. Chem. A **1**, 13597 (2013). Copyright 2013 Royal Society of Chemistry.[93] (b) Computed barriers of C–H bond activation of methane, $E_{a,C-H}$, as a function of the metal-oxo formation energies, ΔE_O. The best-fit line has $r^2 = 0.94$ and a mean absolute error of 0.09 eV. MOFs with $E_{a,C-H} < 1$ eV are classified as being reactive toward C–H bond activation (based on $E_{a,C-H}$ values for cation-exchanged zeolites that can activate methane), and MOFs with $E_{a,C-H} < 0$—as having thermodynamically favored active sites when using O_2 as the reference state. Symbol color refers to the group number of the metal in the periodic table, while the symbol shape indicates the formal oxidation state of the metal site prior to oxidation as 1+ (▲), 2+ (●), or 3+ (■). Reproduced with permission from Rosen et al., ACS Catal. **9**, 3576 (2019). Copyright 2019 American Chemical Society.[167]

13); this prediction was confirmed experimentally, resulting in a world-record performance, 22.5% over the best performing system at the time. The interactive 5D visualization tool for comprehensive data mining is accessible at http://aam.ceb.cam.ac.uk/mof-explorer.

B. Machine learning

While high-throughput screening certainly offers a relatively rapid means to map the large structure–property space of the framework materials, the computational and time costs of the commonly employed GCMC and DFT methods remain a major bottleneck when applied to databases featuring more than 100 000 materials. Moreover, large amounts of data, generated in high-throughput workflows, are, on one hand, challenging to analyze, but, on the other hand, attractive for big-data approaches. This is where machine learning (ML) can accelerate materials discovery by as much as 2–3 orders of magnitude, offering efficient ways to predict the material properties, analyze the structure–property relationships, and even reverse-design new material architectures. Applying machine learning to materials discovery

generally entails (i) preparing a sufficiently large and representative training set containing material structures and computed (e.g., through high-throughput screening) or measured properties, (ii) selecting an appropriate machine-readable representation of a material, (iii) choosing an efficient machine learning model (architecture), and (iv) visualizing and analyzing the results of the ML prediction. In the past 4 years, several review articles have been published on this topic, both focusing on specific applications in gas storage and separation,[174–176] and providing a more general overview of ML methods in this field of research.[177–179] Below we highlight recent and innovative ML approaches to the prediction and design of framework materials hosting molecular guests.

1. Datasets

In addition to the sets of existing and hypothetical MOF structures, for which various properties have been computed with the grand-canonical Monte Carlo and/or density functional theory in a high-throughput manner (see Sec. V A), a set containing experimental and DFT-computed data for 15 713 MOF, entitled QMOF, has been developed by the Snurr group with the specific goals to train and test machine learning models, and to facilitate the discovery of new materials.[180] Using the SOAP similarity kernel for unsupervised dimensionality reduction with a uniform manifold approximation and projection (UMAP) algorithm, the authors constructed an insightful structure (experimental crystal structures)—property [PBE-D3(BJ) computed band gaps] map of QMOF (Fig. 14).

2. Feature selection

Choosing the right descriptor of the material structure and chemistry is crucial to obtain reliable ML predictions for a reasonably sized training set. In 2013, the Woo research group developed an atomic property weighted radial distribution function (AP-RDF) descriptor[181] specifically tailored to gas adsorption in MOFs. The AP-RDF score employs Gasteiger's radial distribution functions, popular in chemoinformatics, and weights them according to atomic electronegativity, polarizability, and van der Waals volume, thus capturing geometric and chemical features simultaneously. Approximately 58 000 structures from the hMOF database were evaluated for their CH_2, N_2, and CO_2 uptake capacity. Both the principal component analysis (PCA) and the quantitative structure–property relationship (QSPR) method using AP-RDF scores were able to correctly identify the high-performing MOFs, with R^2 values for the predicted uptake capacity above 0.7. A webserver implementation of the AP-RDF scores using multilinear regression (MLR) and support vector machine (SVM) learning models for predicting the uptake capacities called MOFIA (MOF Informatics Analysis) was also developed. This tool was subsequently used to discover MOFs with high methane storage capacities based on the interplay of two structural parameters—dominant pore size and void fraction—using a nonlinear support vector machine model [Fig. 15(a)].[182] Similarly, Halder and Singh found the void fraction to be the most significant factor defining the C_2H_6/C_2H_4 selectivity when screening the hMOF database,[183] while Yang and co-workers identified the pore limiting diameter, followed by the largest cavity diameter and porosity, as most important for the gas separation efficiency of existing MOFs using principal component analysis.[184] For the selective adsorption of p-xylene over o- and m-isomers in MOFs,
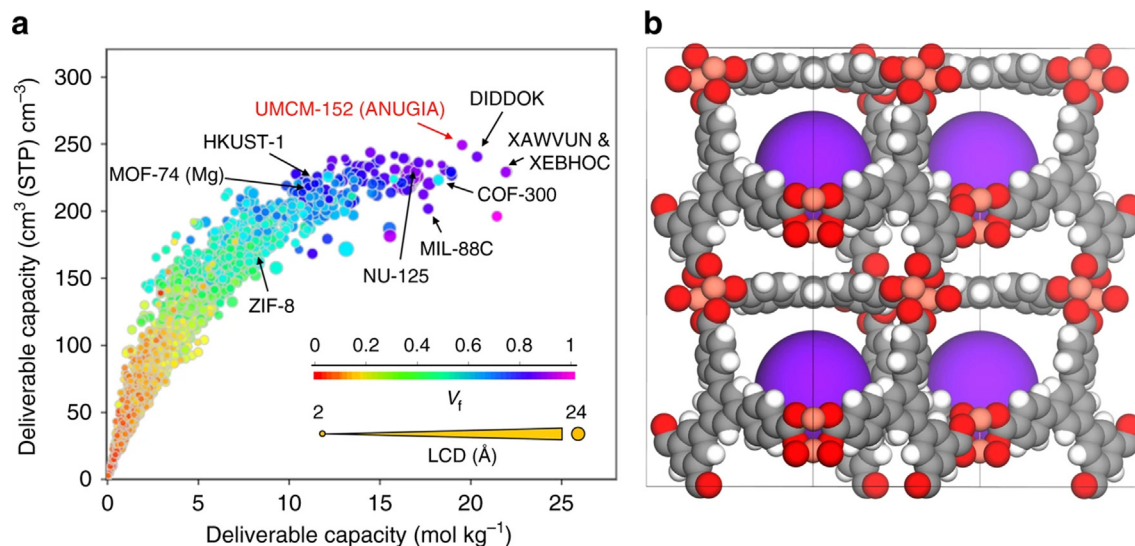
FIG. 13. Top-performing materials for oxygen storage. (a) Oxygen volumetric and gravimetric deliverable capacities (at 140 bar storage and 5 bar release pressures) for 2932 MOF structures at 298 K, color-coded by void fraction. Arrows represent common MOFs and promising materials identified in this work. (b) The crystal structure (supercell $2 \times 2 \times 1$) for the top material identified for volumetric oxygen storage, UMCM-152. Main cavity is represented by a purple sphere. Reproduced with permission from Moghadam *et al.*, Nat. Commun. **9**, 1387 (2018). Copyright 2018 Authors, licensed under a Creative Commons Attribution (CC BY) license.[173]

the pore limiting diameter and largest cavity diameter were again found to me the most important performance descriptors.[185] AP-RDF descriptors were also utilized to screen MOFs for CO_2 capture in conjunction with a classifier machine learning model.[186] Specifically,

instead of training ML to predict the absolute uptake capacities, an SVM with the AP-RDF scores was trained to classify whether a given MOF has low or high CO_2 uptake capacity. Out of 292 050 tested MOFs, only ca. 10% were selected by the classifier for subsequent
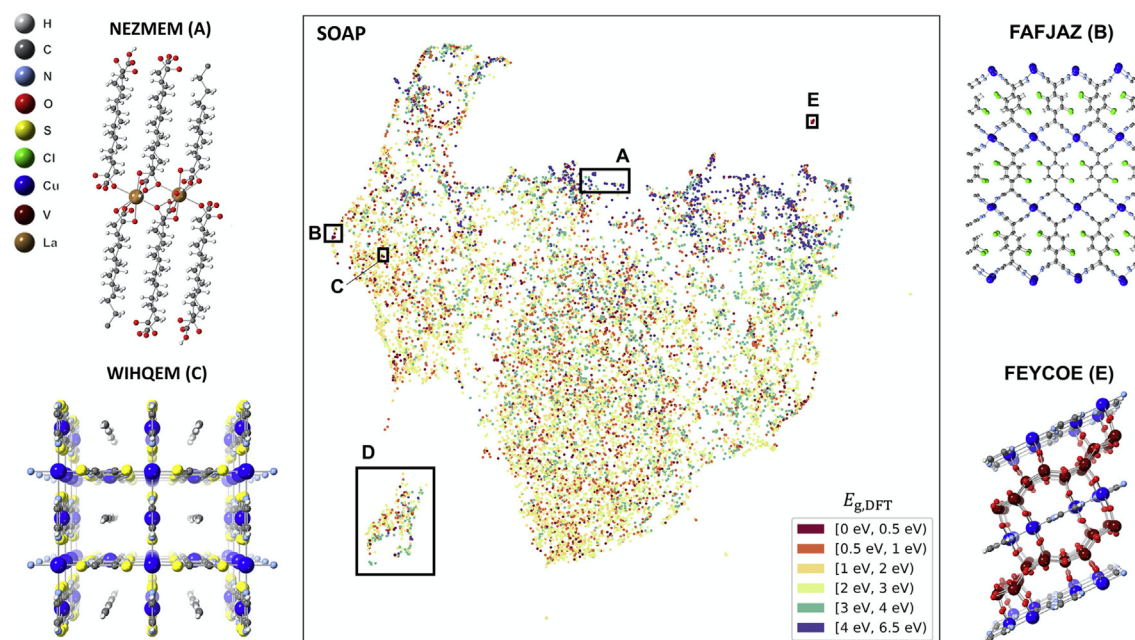
FIG. 14. Compound space of QMOF-14482 database, based on unsupervised structural dimensionality reduction using UMAP and SOAP average similarity kernel of the unrelaxed structures. The PBE-D3(BJ) band gaps of the DFT-optimized structures, $E_{g,DFT}$, are overlaid on the UMAP. Selected MOFs in the projection are highlighted. Reproduced with permission from Rosen *et al.*, Matter **4**, 1578 (2021). Copyright 2021 Authors, licensed under a Creative Commons Attribution (CC BY) license.[180]

TABLE III. Evaluation of predictive performance (R^2 values) of mass-based methane uptake in various MOFs using only structural, only chemical, and both structural and chemical predictors. DT—decision tree, SVM—support vector machine, P—Poisson regression, and RF—random forest. Reproduced with permission from Pardakhti et al., ACS Comb. Sci. **19**, 640 (2017). Copyright 2017 American Chemical Society.[188]

Predictor type	DT	SVM	P	RF
Structural only	0.75	0.81	0.84	0.88
Chemical only	0.34	0.42	0.42	0.65
Structural and chemical	0.84	0.90	0.92	0.97

the type and number of each atom, degree of unsaturation, ratios of the quantities of different atoms, electronegativity, and metallic percentage. Across all tested ML models, a combination of structural and chemical descriptors leads to better prediction of the methane uptake compared to models using descriptors of only one class (Table III). The best results—an R^2 of 0.98 and a mean absolute percent error of about 7%—were achieved with the random forest algorithm, which took approximately 2 h on a single personal computer to train the model and predict adsorption capacity of 130 398 MOFs. The Froudakis group employed a similar concept of ML descriptors for MOFs, based on the types of atoms in the material rather than its building blocks, and also achieved the best performance in predicting methane and carbon dioxide adsorption capacities of 137 953 hypothetical MOFs with a combination of geometric and atom type descriptors.[189] Moreover, a model, trained on MOFs only and using the atom types in addition to the structural descriptors, was able to accurately predict the methane adsorption capacity in 69 839 covalent organic frameworks (Table IV).

3. ML models

Machine learning models come in many flavors.[190] The tree-based methods, such as decision trees (DTs), regression trees (RTs), and random forests (RFs), recursively split the training sample according to simple decision rules. Kernel-based methods, e.g., support vector machines (SVMs), kernel ridge regression (KRR), and Gaussian process regression (GPR), non-linearly transform the inputs into a

FIG. 15. (a) Two-dimensional response surfaces of the SVM models for methane storage in various MOFs at 100 bar using void fraction and dominant pore size. The blue dots represent the GCMC simulated uptake values. The color of the surface represents the methane storage value, from blue (the lowest value) to red (the highest value). Blue and red arrows indicate maxima on the response surface. Reproduced with permission from Fernandez et al., J. Phys. Chem. C **117**, 7681 (2013). Copyright 2013 American Chemical Society.[182] (b) Heatmaps of GBTR-predicted CO_2 working capacity plotted against GCMC-simulated CO_2 working capacity (left), and GBTR-predicted CO_2/H_2 selectivity plotted against GCMC-simulated CO_2/H_2 selectivity (right) for the 358 400 MOFs in the test set. The GBTR model was built using the normalized AP-RDF descriptors weighted by electronegativity, hardness, and van der Waals volume, and 6 geometric descriptors. The colors of the heatmaps correspond to the number of MOFs: red is high and blue is low. Reproduced with permission from Dureckova et al., J. Phys. Chem. C **123**, 4133 (2019). Copyright 2019 American Chemical Society.[187]

high-throughput screening, thus greatly diminishing the associated computational effort. In another study, three AP-RDF descriptors were combined with six geometric descriptors in a gradient boosted trees regression (GBTR) to predict CO_2 working capacities and CO_2/H_2 selectivities of 358 400 hypothetical MOFs with R^2 values of 0.944 and 0.872, respectively [Fig. 15(b)].[187] This approach allowed identifying the 1000 best performing MOFs for CO_2/H_2 separation.

In 2017, Pardakhti et al. appended typical structural descriptors of MOFs (such as density, maximum and dominant pore diameter, void fraction, and gravimetric surface area), computed using Monte Carlo approaches, with various descriptors of the framework's atomic composition, extracted from crystallographic data.[188] These include

TABLE IV. Evaluation of predictive performance (R^2 values) of methane and carbon dioxide adsorption capacities for various nanomaterials. The descriptors used by the ML algorithm were either the structural features of the nanomaterials, alone (second column) or combined with the atom types (third column). In the ML algorithm either the MOFs and COFs databases were used, separately (first two rows) or combined (third row). Finally, the results in the last row were computed by using only MOFs for the training of the ML algorithm, while the obtained ML model was used for predictions in COFs. Reproduced with permission from Fanourgakis et al., J. Am. Chem. Soc. **142**, 3814 (2020). Copyright 2020 American Chemical Society.[189]

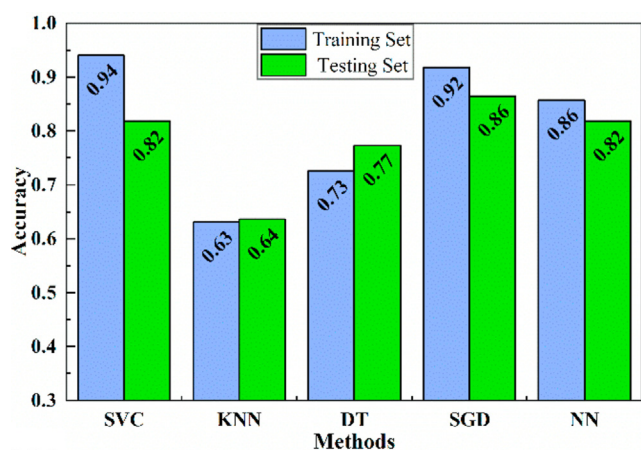| Database	R^2 (struct.)	R^2 (struct. + atom types)
MOFs	0.907	0.960
COFs	0.969	0.981
MOFs + COFs	0.933	0.965
COFs (from MOFs)	0.581	0.878

07 May 2024 15:47:34

higher dimensional space. Finally, artificial neural networks (NNs) are repeated compositions of simple functions, typically arranged in consecutive layers. To identify the best ML model for a specific type of data and chemical problem, several models are often compared in terms of their learning speeds and prediction accuracies. Yang *et al.* evaluated four ML algorithms—DT, RF, SVM, and backpropagation neural network (BPNN)—for predicting the gas separation performance of 6013 computation-ready, experimental metal–organic framework membranes (CoRE-MOFMs) using fivefold cross-validation.[184] Wu and co-workers compared the predictive power of support vector machine, random forest regression, and gradient boosting regression tree models for methane adsorption in 130 397 hypothetical MOFs.[191] In both studies, the random forest algorithm outperformed all other considered ML models. For the training set based on experimental results of CO_2 fixture with MOF catalysts from approximately 100 published papers, SVM, stochastic gradient descent (SGD), and NN models performed better than decision trees and K-nearest neighbor classification models (Fig. 16).[192] Finally, the back-propagation neural network was shown to outperform the partial least-square (PLS) method in predicting the adsorption capacity of organic sulfur gases in 4764 CORE-MOFs after being trained on the hMOF database.[193]

In 2020, the Froudakis group addressed the problem of the model choice by adapting an Automated Machine Learning (AutoML) architecture to train statistical and ML models and estimate their predictive performance for MOFs' chemical properties.[194] This approach allows tuning the hyper-parameters of the ML models and avoids the common issue of overfitting, accurately assessing predictive performance even for relatively small (less than 100 datapoints) sets of experimental data. The pipeline is implemented in the Just Add Data Bio, or JADBio tool, and an illustrative prediction of CO_2 and CH_2 adsorption under various thermodynamic conditions is available at https://app.jadbio.com/share/86477fd7-d467-464d-ac41-fcbb0475444b.

Very recently, Van Speybroeck and co-workers developed an approach for constructing machine learning potentials (MLPs) for MOFs.[195] In contrast to ot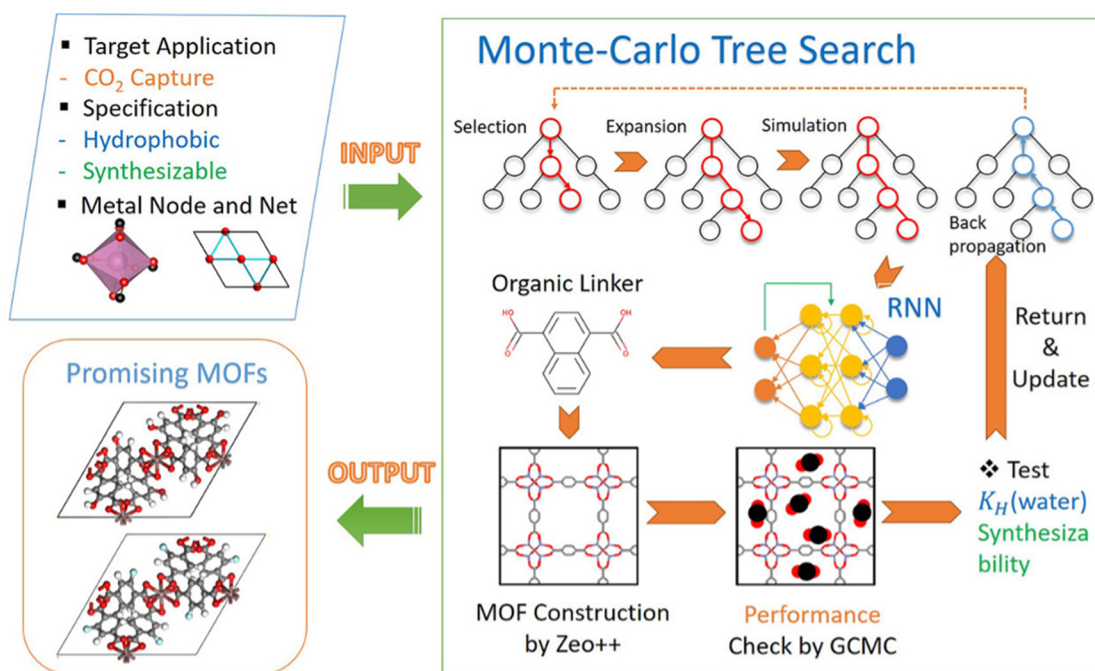her MLP construction techniques that require costly molecular dynamics trajectories at the density functional theory level as training data, this new incremental learning scheme employs machine learning potentials to generate the training data, metadynamics to ensure broad sampling of the phase space, and a message passing neural network for efficient on-the-fly learning. In this manner, accurate and transferrable ML potentials for MOFs can be generated from as little as a few hundred single-point DFT computations.

4. Screening and design workflows

Automated workflows combining high-throughput screening with machine learning prediction offer unparallel speed of materials discovery. For example, Wand *et al.* combined hierarchical screening of the CORE-MOF database based using GCMC simulations with the crystal graph convolutional neural networks algorithm to develop a predictive model of methane adsorption (Fig. 17).[196] This model was transferred to randomly selected covalent organic frameworks and zeolitic imidazolate framework materials, as well as to the hMOF database, in which a material with the maximum working capacity close to the Department of Energy's 2015 target was discovered. Reverse design of a metal–organic framework for efficient CO_2 capture in humid conditions was achieved by Zhang and co-workers.[197] 27 combinations of metal nodes and framework topologies were screened using a combination of Monte Carlo tree search (MCST) and recurrent neural network (RNN) using three performance descriptors: high adsorption performance, experimental accessibility, and good hydrophobicity. Several newly designed systems were found to display a good trade-off between adsorption selectivity and uptake capacity whilst being sufficiently hydrophobic and synthetically viable. Very recently, Chen and co-workers screened several experimental and hypothetical databases in search of MOFs with open Cu sites for efficient isobutene/isobutane separation.[198] Configuration-bias Monte Carlo was used to simulate adsorption, and molecular dynamics—diffusion of the hydrocarbons in MOFs. The generated data were then used to train five ML models in conjunction with seven physical descriptors to predict the separation performance of MOFs. Finally, a materials-genomics strategy was applied to identify the best-performing genes (nodes and linkers) and cross-assemble them into novel MOFs. On this basis, five MOFs—four from the screened databases and one newly assembled—were found to have high thermal stability, isobutene uptake, and isobutene/isobutane selectivity. Stable adsorption configurations of these candidates were verified using GGA and hybrid DFT computations.

VI. YOUTH LEAGUE: COVALENT ORGANIC FRAMEWORKS

Covalent organic frameworks are relatively recent, metal-free analogues of MOFs, offering a number of advantages over their famous ancestors while retaining the large internal surface area, ordered pores, structural diversity, tunable functionalization, and the ability to absorb, store, and release guest molecules. Compared to MOFs, COFs are more lightweight, environmentally sustainable, and thermally stable. Whereas MOFs can form relatively strong interactions with guest molecules via their empty metal sites, the host–guest interactions in COFs are exclusively non-covalent. Many COFs consist of 2D layers of covalently connected nodes and linkers, which are assembled in the third dimension via non-covalent interactions. The stacking of the 2D layers is crucial for the properties of the COF[199] yet

FIG. 16. Accuracy scores of five ML algorithms on training and test sets for methane adsorption in MOFs. Adapted with permission from Li *et al.*, J. Materiomics **7**, 1029 (2021). Copyright 2021 Authors, licensed under a Creative Commons Attribution-Non Commercial-No Derivatives (CC BY NC ND) license.[192]

FIG. 17. Design algorithm for application-specific metal–organic frameworks. Target application and type of metal node and net are the inputs, organic linkers generated by ChemTS combining the MCTS and RNN are the outputs. A new MOF constructed using Zeo++ undergoes a performance check for the target application; internal parameters in MCTS are then updated. Reproduced with permission from Wang et al., ACS Appl. Mater. Interfaces **12**, 52797 (2020). Copyright 2020 American Chemical Society.[196]

is difficult to determine.[200,201] While the x-ray diffraction is the predominant method to structurally characterize COF crystals, the diffraction peaks represent an average over the measured portion of the crystal and, therefore, random layer offsets are difficult to determine and to distinguish from eclipsed stacking. The structural characterization of COFs is further complicated by the difficulty of growing single crystals suitable for single crystal x-ray diffraction. Thus, they are often characterized with powder XRD. Even more challenging is the structure determination of COFs encapsulating guest molecules. Consequently, even though a few experimentally determined host-guest structures exist for MOFs, to the best of our knowledge, none have been reported for COFs.

Methodological approaches to the modeling of host–guest interactions in COFs are fairly similar to those used for MOFs, e.g., density functional theory and other *ab initio* methods, molecular dynamics and Monte Carlo simulations, as well as their multiscale combinations.[202] The absence of the metal atoms has several important implications for the modeling of COFs. On the one hand, it alleviates the need to employ relativistic and Hubbard U-corrections. On the other hand, the choice of the cluster model is less intuitive than in MOFs and requires cleaving covalent single and even double bonds.[203,204]

Classical molecular dynamics simulations, often combined with periodic DFT modeling, were employed to investigate the interactions of COFs with anticancer drugs 5-fluorouracil[205] and quercetin,[206] pollutant bisphenol A [Fig. 18(a)],[207] to rationalize the separation of CO_2/N_2 mixtures in a 2D-COF,[208] and to explain the ultrahigh adsorption affinity for dispersed anionic pollutants in a new three-dimensional framework, 3DCOF-g-VBPPh3Cl [Fig. 18(b)].[209] *Ab initio* molecular

dynamics simulations are often evoked to elucidate the interaction sites and to estimate the temperature- and pressure-dependent loading capacities of COFs, particularly for hydrogen storage applications [Fig. 18(c)].[210–212]

Grand canonical Monte Carlo simulations remain the method of choice for modeling the dynamical behavior of COFs upon guest capture and/or release. Tong *et al.* combined GCMC and configurational bias MC with cluster and periodic DFT computations to investigate the structure–property relationships across a diverse set of 46 COFs for CO_2 capture.[208] Large "adsorbility" of adsorbates was put forward as a promising descriptor of the framework's separation performance. Using a similar multiscale approach, Das and Mandal explained the selectivity of a triazine-based benz-bis(imidazole)-bridged COF (TBICOF) toward CO_2 over N_2 and CH_4 [Fig. 19(a)], and toward benzene over cyclohexane.[213] Chen and co-workers supplemented periodic DFT and GCMC simulations with the extended transition state—natural orbitals for chemical valence (ETS-NOCV) analysis to study the selectivity of a diamond-topology covalent organic framework, COF-300 (*dia-c5*), toward various C4 hydrocarbons [Fig. 19(b)].[214] Diverse topological parameters of the framework were found to be useful in tuning the selectivity and predicting the material's synthesizability. Metropolis Monte Carlo together with periodic DFT were used to investigate the adsorption of environmental pollutants—polybrominated diphenyl ethers—in a reticulated framework, TAPT-DMTA-COF.[215]

Several databases of COF structures have been published to enable the high-throughput screening of these materials for specific applications. In 2017, the Zhong group introduced[216] and in 2018 updated[217] a computation-ready, experimental covalent organic
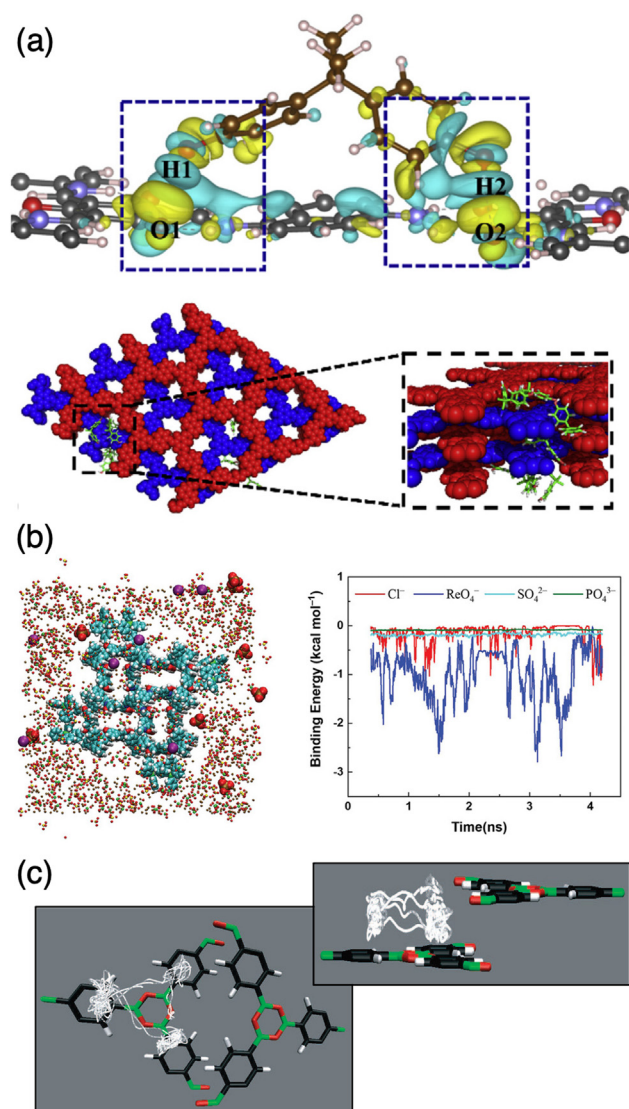
FIG. 18. (a) The differential charge density of bisphenol A on the surface of TpND COF (top) and MD simulation of adsorption of 10 bisphenol A molecules onto TpND COF at 200 ns (bottom). Reproduced with permission from Wei *et al.*, J. Mol. Liq. **301**, 112431 (2020). Copyright 2020 Elsevier B.V.[207] (b) A snapshot from MD trajectories of ReO_4^- adsorption in 3DCOF-g-VBPPh$_3$Cl (left) and computed average binding energies of 3DCOF-g-VBPPh$_3$Cl with the four anions in aqueous solution (right). Reproduced with permission from Wang *et al.*, Adv. Funct. Mater. **32**, 2205222 (2022). Copyright 2022 Wiley-VCH GmbH.[209] (c) *Ab initio* molecular dynamics trajectories (in white) of H atoms of a single H_2 molecule within COF-1 at 150 K, top (left) and side (right) views. Reproduced with permission from Srepusharawoot *et al.*, J. Phys. Chem. C **113**, 8498 (2009). Copyright 2009 American Chemical Society.[212]

framework (CoRE COF) database, which includes almost all existing experimental structures. A year later, the database was updated with new structures. The solvent-free and disorder-free structure files of over 280 COFs in 12 topologies are publicly available online at https://core-cof.github.io/CoRE-COF-Database/. Evaluating the structures in

the CoRE COF database for CH_4 delivery, the authors showed that the top performing systems have large volumetric surfaces and the pore channels are passable in three dimensions.[217] Aksu *et al.* screened CoRE-COF for CO_2/H_2 separation by evaluating the CO_2 and H_2 permeabilities and selectivities of COF membranes using a combination of MD and GCMC.[218] Materials with narrow pores and low porosities were found to be best for separating CO_2 from H_2, while COFs with the opposite characteristics efficiently separate H_2 from CO_2. Using a similar computational setup, this research group also demonstrated that COFs outperform conventional adsorbents (zeolites and activated carbons) in terms of selectivity of CO_2 separation from flue gas and offer better working capacities than MOFs.[219] In 2019, the Smit group went beyond the "CoRE" approach, introducing a set of over 300 CURATED (Clean, Uniform, and Refined with Automatic Tracking from Experimental Database) COFs together with DFT geometries and point charges, available at https://www.materialscloud.org/discover/curated-cofs.[220] A workflow for screening this database for promising CO_2 adsorbents was also developed and encoded in the Automated Interactive Infrastructure and Database for Computational Science (AiiDA).[221]

In 2018, the Smit group presented a database of 69 840 hypothetical covalent organic frameworks built from 666 organic linkers and four established synthetic routes.[222] The database was screened for methane storage capacities with GCMC, resulting in a top performer, composed of carbon-carbon bonded triazine linkers in the *tbd* topology, with a deliverable capacity beating the best existing methane storage materials. Optimal values for several topological features of the frameworks, including density and surface area, were proposed to achieve the best adsorbed natural gas storage performance (Fig. 20). This database was also screened by the Smit group for carbon capture using parasitic energy as a key performance descriptor.[223] Out of over 69 000 hypothetical COFs, more than 70 outperformed the best experimental COFs, and several performed similarly to Mg-MOF-74. Finally, Lan and co-workers presented a methodology for a high-throughput construction of covalent organic frameworks based on the materials genomics strategy mimicking their natural growth processes.[224] From a library of 130, a database of ca. 470 000 COFs with known and ten new topologies was constructed. Two three-dimensional COFs with a novel *ffc* topology were successfully synthesized.

In 2023, a Ready-to-use and Diverse Database of Covalent Organic Frameworks with Force field based Energy Evaluation (ReDD-COFFEE) was published and made freely available via Materials Cloud (https://doi.org/10.24435/materialscloud:nw-3j).[225] It contains 268 687 DFT-optimized hypothetical COF structures together with bespoke force field parameters for each framework. The structures were generated from 279 diverse secondary building blocks, arranged in 1114 distinct two- and three-dimensional topologies; only structurally stable and likely synthesizable systems were included in ReDD-COFFEE. System-specific periodic force fields were obtained from cluster force fields, derived in turn for each SBU by fitting to *ab initio* data, and were shown to outperform a popular generic UFF in describing the crystal structures of several experimentally characterized COFs. Finally, a subset of 10 000 structures from ReDD-COFFEE was screened using GCMC for vehicular methane storage, yielding candidates with outstanding volumetric deliverable capacities.

07 May 2024 15:47:34
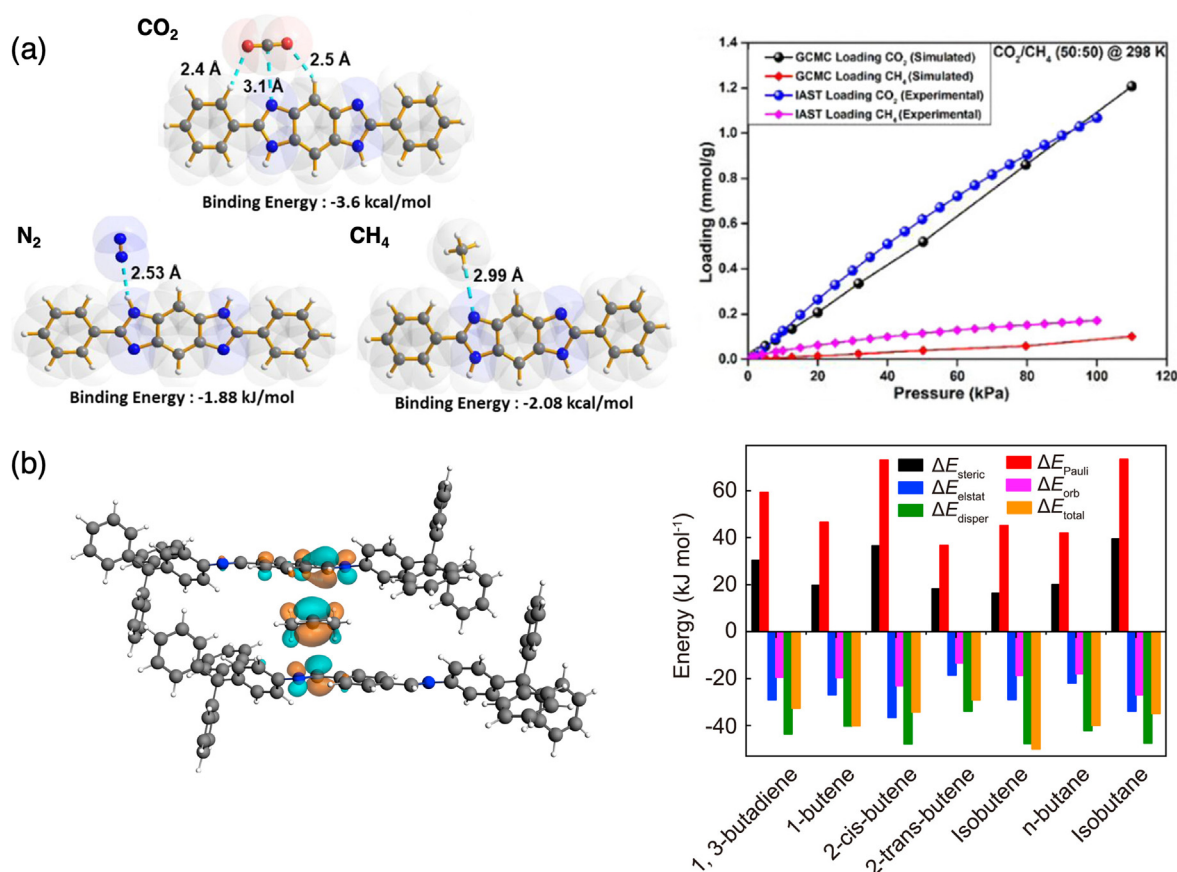
FIG. 19. (a) B3LYP/6-31G+(d,p) optimized geometries of the benz-bis(imidazole) repeating unit of TBICOF with CO_2, N_2, and CH_4 (left), and simulated and experimental loading amounts in TBICOF in a mixed gas phase (right). Reproduced with permission from P. Das and S. K. Mandal, Chem. Mater. **31**, 1584 (2019). Copyright 2019 American Chemical Society.[213] (b) The most contributing NOCV orbitals (0.03 a.u. isovalue) in the host–guest interaction between isobutene and COF-300 (left) and the energy decomposition analysis of the host–guest interactions between C4 hydrocarbons and COF-300 (dia-c5, right). Adapted with permission from Chen *et al.*, Green Energy Environ. **7**, 296 (2021). Copyright 2021 Authors, licensed under a Creative Commons Attribution-Non Commercial-No Derivatives (CC BY NC ND) license.[214]

VII. CONCLUSIONS AND OUTLOOK

In silico modeling of the host–guest complexes between organic framework materials and their molecular guests, such as gases, small hydrocarbons, and therapeutics, offers valuable insight into the dynamic and static, structural and electronic aspects of the host–guest interactions, which can be used to rationalize experimental observations and identify the best performing systems (Fig. 21). Molecular dynamics and Monte Carlo methods allow modeling guest diffusion through and adsorption in the framework's pores, simulating the adsorption isotherms and evaluating the loading capacities. Periodic density functional theory with dispersion, Hubbard U (for MOFs), and thermal corrections provides refined structures and heats of adsorption, while cluster models treated with more accurate DFT, post-HF, and multireference methods yield information about the precise physical nature of the interactions, reaction mechanisms, and response properties of the framework–guest complexes. Interaction analysis and partitioning schemes deliver a fundamental understanding of the role of the framework's building blocks and functionalization. Employing some of these modeling techniques in a multiscale

manner, high-throughput screening and machine learning are performed on the databases of existing and hypothetical framework materials to not only rank the candidates according to their performance in a given application, but also to elucidate the structural parameters determining performance, thus opening the doors toward tuning of the known and reverse-designing the new MOFs and COFs.

If computational modeling is so powerful, then why have not the best (most stable, lightweight, sustainable, high-capacity, responsive) organic frameworks been already developed for applications in molecular capture, separation, transport, storage, catalysis, etc.? For one, this area of research is plagued by the common dilemma of *in silico* modeling: realistic representation of the system vs accuracy of the theoretical approach. No method is capable of describing large, periodic frameworks hosting numerous guest molecules under relevant conditions (solvent, pH, pressure, temperature, irradiation, etc.) across practically relevant timescales whilst fully taking into account static and dynamic correlation, non-adiabaticity, relativistic effects, and many other challenging aspects of the electronic structure. Whether all these factors are important, and to what extent, strongly depends on the
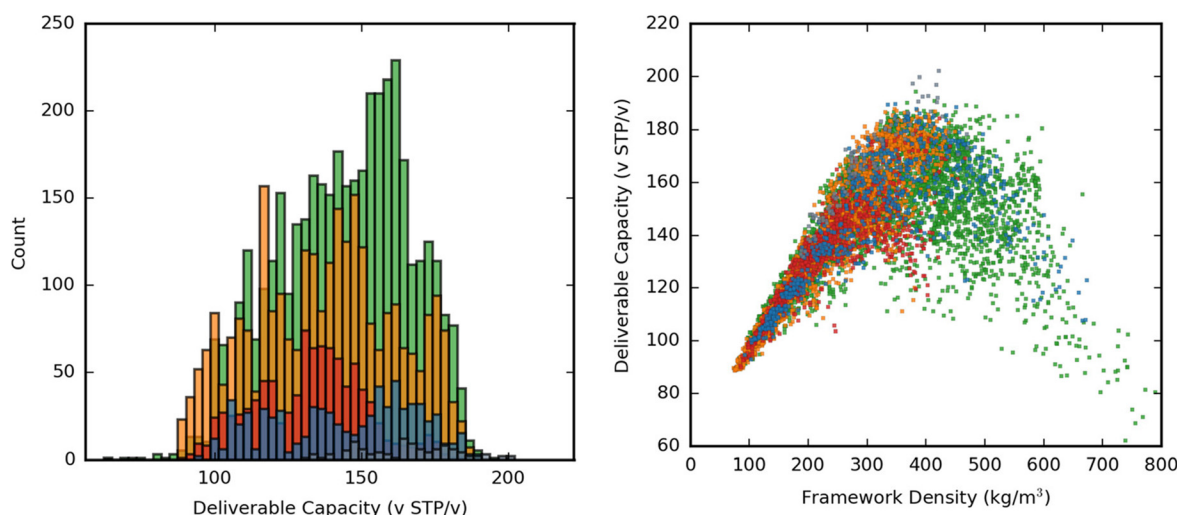
FIG. 20. Computed deliverable capacities at 298 K and 65 bar for methane storage in hypothetical 2D COFs, plotted as a histogram (left) and vs the framework densities (right). Color key: blue = amide, red = amine, orange = imine, green = C–C, gray = mixed. Reproduced with permission from Mercado *et al.*, Chem. Mater. **30**, 5069 (2018). Copyright 2018 Authors, licensed under an ACS Author Choice license.[222]

investigated host-guest system. Cluster models address some of these methodological problems but sacrifice realistic system representation and necessitate cluster selection—a procedure so far lacking well defined rules and automatized implementations. With a few notable exceptions,[226–230] energy decomposition and density and wavefunction partitioning schemes, helpful in understanding the intricacies of the host–guest interactions, remain limited to these finite and relatively small cluster models. Similarly, predictions of the influence of guest occlusion on the solid-state properties of the frameworks, such as their band structures and densities of states, remain scarce. Large realistic
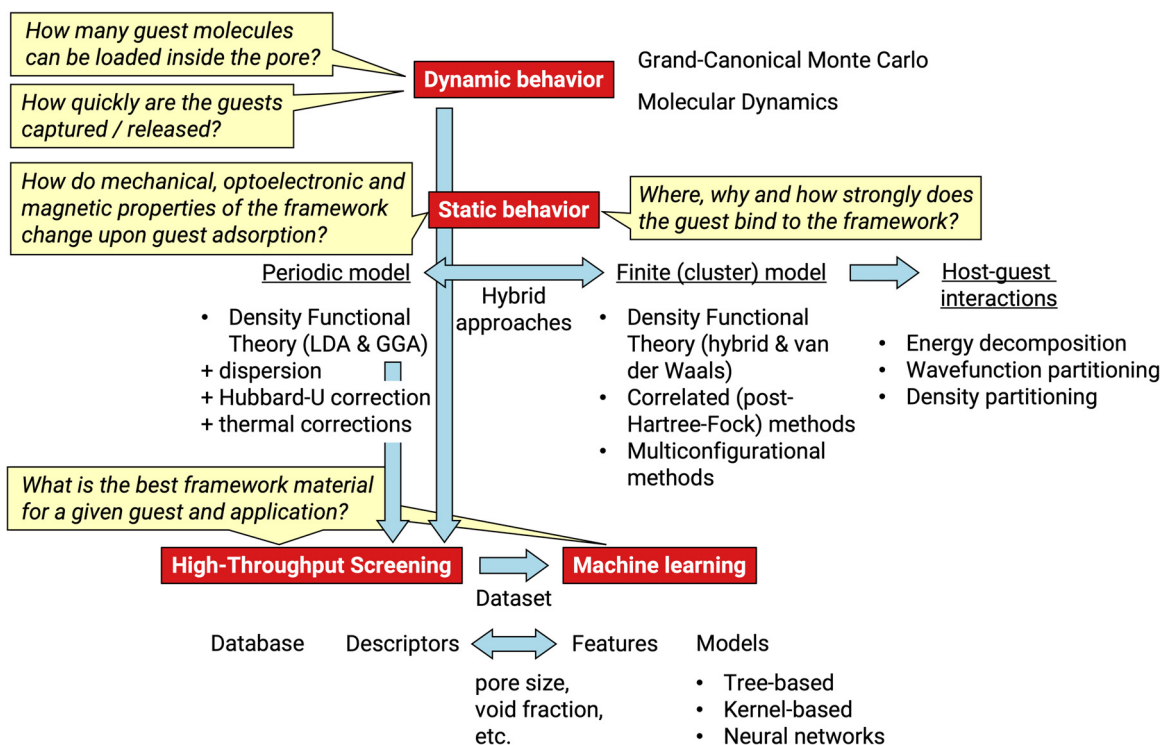
FIG. 21. Key questions, addressed by the modeling of the host–guest interactions in framework materials, and the corresponding *in silico* approaches.

models are treatable with molecular mechanics force fields and GGA and LDA DFT methods; however, using these "cheaper" approaches often leads to compromised numerical accuracy. Since it is rarely computationally feasible to perform accurate high-level electronic structure theory computations on large, realistic models, the reliability of the various approximations can only be verified against experimental data. The latter is generally limited, preventing across-the-board validation of these methods. For the same reason, high-throughput screening and machine learning predictions utilize computational rather than experimental data and are, therefore, subject to the same error bars as the underlying *in silico* methods. Moreover, databases of experimental structures, fed into HTS and ML, are often biased toward high-performance materials. Insufficient sampling in the regions of chemical space containing low-performing and experimentally overlooked organic frameworks compromises the reliability of machine learning when it is used to predict the properties of novel and unconventional materials. Finally, the disconnect between theory and experiment is perhaps most pronounced in the practical viability of *in silico* predicted materials, which are often "good on paper" (in a computer), but are unstable, hard or impossible to manufacture, especially at scale, etc.

In the light (or, more appropriately, the gloom) of the previous paragraph, is there no hope for the computationally designed breakthrough for organic frameworks supporting tailored interactions with molecular guests? In this Review, we have collected illustrative, successful recipes from the literature for addressing the aforementioned challenges. Individual simulation techniques, restricted to specific system sizes and timescales at a given accuracy, are combined in multi-level and multiscale approaches balancing large system sizes with reliable predictions. Computations on thousands of framework materials using multiple codes are facilitated by automated workflows, and their results are shared freely and openly via community-ran repositories. Together with unbiased databases of hypothetical MOF and COF structures, published in open access, they are actively used in training machine learning models, which can predict not only the interaction features and performance metrics, but even the synthesizability of the frameworks.[231–234] With accurate quantum-chemical insight on one side and big-data analysis on the other, precise design guidelines based on the compositional and topological parameters of the frameworks are elucidated. Ultimately, they yield predictions of candidate materials with outstanding performances, at times overtaking the best systems in use at the time. Occasionally, these predictions are subsequently validated by experiment.

Which challenges should be tackled next? In our opinion, automated cluster selection will substantially facilitate the computational analysis of the host–guest interactions in organic frameworks and is likely to benefit greatly from cross-disciplinary approaches. Furthermore, community standards for *in silico* generated data, including metadata records, will enable post-processing and reuse of these data in future high-throughput and machine learning studies, significantly saving computational resources and time whilst simultaneously expanding the training sets in size and heterogeneity. Similarly, more experimental data, especially measured on a range of systems under identical conditions, as well as reporting of the "failed" experiments, will allow broader benchmarking of the methods and development of more universally applicable predictive models. Ultimately, the key to the continuing success in the rapidly growing

field of metal–organic and covalent organic framework adsorbents, filters, catalysts, and delivery agents is in communication between the main players—method developers, computational materials scientists, and experimentalists.

AUTHOR DECLARATIONS

Conflict of Interest

The authors have no conflicts to disclose.

Author Contributions

Michelle Ernst: Conceptualization (equal); Visualization (supporting); Writing – original draft (lead); Writing – review & editing (equal). **Jack Evans:** Writing – review & editing (equal). **Ganna Gryn'ova:** Conceptualization (equal); Funding acquisition (lead); Supervision (lead); Visualization (lead); Writing – original draft (supporting); Writing – review & editing (equal).

DATA AVAILABILITY

Data sharing is not applicable to this article as no new data were created or analyzed in this study.

REFERENCES

[1]N. Sanchez, R. Fayne, and B. Burroway, "Charcoal: An ancient material with a new face," Clin. Dermatol. **38**, 262–264 (2020).

[2]J. Stenhouse, "On the economical applications of charcoal to sanitary purposes," Br. Foreign Med.-Chir. Rev. **16**, 151–152 (1855).

[3]O. M. Yaghi, D. A. Richardson, G. Li, C. E. Davis, and T. L. Groy, "Open-framework solids with diamond-like structures prepared from clusters and metal-organic building blocks," MRS Proc. **371**, 15 (1994).

[4]A. P. Côté, A. I. Benin, N. W. Ockwig, M. O'Keeffe, A. J. Matzger, and O. M. Yaghi, "Porous, crystalline, covalent organic frameworks," Science **310**, 1166–1170 (2005).

[5]Y. Yan, S. Yang, A. J. Blake, and M. Schröder, "Studies on metal-organic frameworks of Cu(II) with isophthalate linkers for hydrogen storage," Acc. Chem. Res. **47**, 296–307 (2014).

[6]L. J. Murray, M. Dinc, and J. R. Long, "Hydrogen storage in metal-organic frameworks," Chem. Soc. Rev. **38**, 1294–1314 (2009).

[7]Y. He, W. Zhou, G. Qian, and B. Chen, "Methane storage in metal-organic frameworks," Chem. Soc. Rev. **43**, 5657–5678 (2014).

[8]J. R. Li, J. Sculley, and H. C. Zhou, "Metal-organic frameworks for separations," Chem. Rev. **112**, 869–932 (2012).

[9]F. Y. Yi, D. Chen, M. K. Wu, L. Han, and H. L. Jiang, "Chemical sensors based on metal–organic frameworks," ChemPlusChem **81**, 675–690 (2016).

[10]G. Xu, P. Nie, H. Dou, B. Ding, L. Li, and X. Zhang, "Exploring metal organic frameworks for energy storage in batteries and supercapacitors," Mater. Today **20**, 191–209 (2017).

[11]E. Barea, C. Montoro, and J. A. R. Navarro, "Toxic gas removal-metal-organic frameworks for the capture and degradation of toxic gases and vapours," Chem. Soc. Rev. **43**, 5419–5430 (2014).

[12]A. Uzun and S. Keskin, "Site characteristics in metal organic frameworks for gas adsorption," Prog. Surf. Sci. **89**, 56–79 (2014).

[13]K. Sumida, D. L. Rogow, J. A. Mason, T. M. McDonald, E. D. Bloch, Z. R. Herm, T.-H. Bae, and J. R. Long, "Carbon dioxide capture in metal–organic frameworks," Chem. Rev. **112**, 724–781 (2012).

[14]A. Dhakshinamoorthy, A. Santiago-Portillo, A. M. Asiri, and H. Garcia, "Engineering UiO-66 metal organic framework for heterogeneous catalysis," ChemCatChem **11**, 899–923 (2019).

[15]J. Gascon, A. Corma, F. Kapteijn, and F. X. Llabrés I Xamena, "Metal organic framework catalysis: Quo vadis?," ACS Catal. **4**, 361–378 (2014).

[16]A. Corma, H. García, and F. X. Llabrés I Xamena, "Engineering metal organic frameworks for heterogeneous catalysis," Chem. Rev. **110**, 4606–4655 (2010).

[17]A. Dhakshinamoorthy, Z. Li, and H. Garcia, "Catalysis and photocatalysis by metal organic frameworks," Chem. Soc. Rev. **47**, 8134–8172 (2018).

[18]L. E. Kreno, K. Leong, O. K. Farha, M. Allendorf, R. P. Van Duyne, and J. T. Hupp, "Metal-organic framework materials as chemical sensors," Chem. Rev. **112**, 1105–1125 (2012).

[19]P. Kumar, A. Deep, and K. H. Kim, "Metal organic frameworks for sensing applications," TrAC - Trends Anal. Chem. **73**, 39–53 (2015).

[20]Z. Hu, B. J. Deibert, and J. Li, "Luminescent metal-organic frameworks for chemical sensing and explosive detection," Chem. Soc. Rev. **43**, 5815–5840 (2014).

[21]S. Keskin and S. Kizilel, "Biomedical applications of metal organic frameworks," Ind. Eng. Chem. Res. **50**, 1799–1812 (2011).

[22]P. Horcajada, R. Gref, T. Baati, P. K. Allan, G. Maurin, P. Couvreur, G. Férey, R. E. Morris, and C. Serre, "Metal–organic frameworks in biomedicine," Chem. Rev. **112**, 1232–1268 (2012).

[23]J. L. Mancuso, A. M. Mroz, K. N. Le, and C. H. Hendon, "Electronic structure modeling of metal-organic frameworks," Chem. Rev. **120**, 8641–8715 (2020).

[24]V. Bernales, M. A. Ortuño, D. G. Truhlar, C. J. Cramer, and L. Gagliardi, "Computational design of functionalized metal-organic framework nodes for catalysis," ACS Cent. Sci. **4**, 5–19 (2018).

[25]J. S. Lee, B. Vlaisavljevich, D. K. Britt, C. M. Brown, M. Haranczyk, J. B. Neaton, B. Smit, J. R. Long, and W. L. Queen, "Understanding small-molecule interactions in metal-organic frameworks: Coupling experiment with theory," Adv. Mater. **27**, 5785–5796 (2015).

[26]Y. Yan, L. Zhang, S. Li, H. Liang, and Z. Qiao, "Adsorption behavior of metal-organic frameworks: From single simulation, high-throughput computational screening to machine learning," Comput. Mater. Sci. **193**, 110383 (2021).

[27]R. Krishna and J. M. van Baten, "In silico screening of zeolite membranes for CO₂ capture," J. Membr. Sci. **360**, 323–333 (2010).

[28]S. S. Han, J. L. Mendoza-Cortés, and W. A. Goddard, "Recent advances on simulation and theory of hydrogen storage in metal–organic frameworks and covalent organic frameworks," Chem. Soc. Rev. **38**, 1460–1476 (2009).

[29]T. Düren, Y. S. Bae, and R. Q. Snurr, "Using molecular simulation to characterise metal-organic frameworks for adsorption applications," Chem. Soc. Rev. **38**, 1237–1247 (2009).

[30]J. D. Evans, K. E. Jelfs, G. M. Day, and C. J. Doonan, "Application of computational methods to the design and characterisation of porous molecular materials," Chem. Soc. Rev. **46**, 3286–3301 (2017).

[31]J. Jiang, R. Babarao, and Z. Hu, "Molecular simulations for energy, environmental and pharmaceutical applications of nanoporous materials: From zeolites, metal–organic frameworks to protein crystals," Chem. Soc. Rev. **40**, 3599–3612 (2011).

[32]R. B. Getman, Y. S. Bae, C. E. Wilmer, and R. Q. Snurr, "Review and analysis of molecular simulations of methane, hydrogen, and acetylene storage in metal-organic frameworks," Chem. Rev. **112**, 703–723 (2012).

[33]Q. Yang, D. Liu, C. Zhong, and J. R. Li, "Development of computational methodologies for metal-organic frameworks and their application in gas separations," Chem. Rev. **113**, 8261–8323 (2013).

[34]R. Krishna, "Diffusion in porous crystalline materials," Chem. Soc. Rev. **41**, 3099–3118 (2012).

[35]G. W. King, "Monte-Carlo method for solving diffusion problems," Ind. Eng. Chem. **43**, 2475–2478 (1951).

[36]L. Zhang, Z. Hu, and J. Jiang, "Sorption-induced structural transition of zeolitic imidazolate framework-8: A hybrid molecular simulation study," J. Am. Chem. Soc. **135**, 3722–3728 (2013).

[37]D. Wu, G. Maurin, Q. Yang, C. Serre, H. Jobic, and C. Zhong, "Computational exploration of a Zr-carboxylate based metal–organic framework as a membrane material for CO₂ capture," J. Mater. Chem. A **2**, 1657–1661 (2014).

[38]J. P. Dürholt, G. Fraux, F. X. Coudert, and R. Schmid, "Ab initio derived force fields for zeolitic imidazolate frameworks: MOF-FF for ZIFs," J. Chem. Theory Comput. **15**, 2420–2432 (2019).

[39]A. K. Rappé, C. J. Casewit, K. S. Colwell, W. A. Goddard, and W. M. Skiff, "UFF, a full periodic table force field for molecular mechanics and molecular dynamics simulations," J. Am. Chem. Soc. **114**, 10024–10035 (1992).

[40]M. A. Addicoat, N. Vankova, I. F. Akter, and T. Heine, "Extension of the universal force field to metal-organic frameworks," J. Chem. Theory Comput. **10**, 880–891 (2014).

[41]D. E. Coupry, M. A. Addicoat, and T. Heine, "Extension of the universal force field for metal–organic frameworks," J. Chem. Theory Comput. **12**, 5215–5225 (2016).

[42]R. Krishna, "Describing the diffusion of guest molecules inside porous structures," J. Phys. Chem. C **113**, 19756–19781 (2009).

[43]J. T. Bullerjahn, S. von Bülow, and G. Hummer, "Optimal estimates of self-diffusion coefficients from molecular dynamics simulations," J. Chem. Phys. **153**, 024116 (2020).

[44]A. I. Skoulidas and D. S. Sholl, "Self-diffusion and transport diffusion of light gases in metal-organic framework materials assessed using molecular dynamics simulations," J. Phys. Chem. B **109**, 15760–15768 (2005).

[45]Y. Yang and D. S. Sholl, "A systematic examination of the impacts of MOF flexibility on intracrystalline molecular diffusivities," J. Mater. Chem. A **10**, 4242–4253 (2022).

[46]D. Dubbeldam, S. Calero, D. E. Ellis, and R. Q. Snurr, "RASPA: Molecular simulation software for adsorption and diffusion in flexible nanoporous materials," Mol. Simul. **42**, 81–101 (2016).

[47]T. Pham and B. Space, "Insights into the gas adsorption mechanisms in metal–organic frameworks from classical molecular simulations," Top. Curr. Chem. **378**, 215–216 (2020).

[48]J. Jiang, S. I. Sandler, M. Schenk, and B. Smit, "Adsorption and separation of linear and branched alkanes on carbon nanotube bundles from configurational-bias Monte Carlo simulation," Phys. Rev. B **72**, 045447 (2005).

[49]D. Damasceno Borges, P. Normand, A. Permiakova, R. Babarao, N. Heymans, D. S. Galvao, C. Serre, G. De Weireld, and G. Maurin, "Gas adsorption and separation by the al-based metal–organic framework MIL-160," J. Phys. Chem. C **121**, 26822–26832 (2017).

[50]Y. Li, X. Wang, D. Xu, J. D. Chung, M. Kaviany, and B. Huang, "H₂O adsorption/desorption in MOF-74: Ab initio molecular dynamics and experiments," J. Phys. Chem. C **119**, 13021–13031 (2015).

[51]M. V. Parkes, J. A. Greathouse, D. B. Hart, D. F. Sava Gallis, and T. M. Nenoff, "Ab initio molecular dynamics determination of competitive O₂ vs. N₂ adsorption at open metal sites of M₂(dobdc)," Phys. Chem. Chem. Phys. **18**, 11528–11538 (2016).

[52]E. Eisbein, J. Joswig, and G. Seifert, "Proton conduction in a MIL-53(Al) metal–organic framework: Confinement versus host/guest interaction," J. Phys. Chem. C **118**, 13035–13041 (2014).

[53]D. L. Chen, S. Wu, P. Yang, S. He, L. Dou, and F. F. Wang, "Ab initio molecular dynamic simulations on Pd clusters confined in UiO-66-NH₂," J. Phys. Chem. C **121**, 8857–8863 (2017).

[54]P. Kanoo, S. K. Reddy, G. Kumari, R. Haldar, C. Narayana, S. Balasubramanian, and T. K. Maji, "Unusual room temperature CO₂ uptake in a fluoro-functionalized MOF: Insight from Raman spectroscopy and theoretical studies," Chem. Commun. **48**, 8487–8489 (2012).

[55]S. Barman, A. Khutia, R. Koitz, O. Blacque, H. Furukawa, M. Iannuzzi, O. M. Yaghi, C. Janiak, J. Hutter, and H. Berke, "Synthesis and hydrogen adsorption properties of internally polarized 2,6-azulenedicarboxylate based metal-organic frameworks," J. Mater. Chem. A **2**, 18823–18830 (2014).

[56]P. Suksaengrat, V. Amornkitbamrung, P. Srepusharawoot, and R. Ahuja, "Density functional theory study of hydrogen adsorption in a Ti-decorated Mg-based metal-organic framework-74," ChemPhysChem **17**, 879–884 (2016).

[57]S. Barman, A. Remhof, R. Koitz, M. Iannuzzi, O. Blacque, Y. Yan, T. Fox, J. Hutter, A. Züttel, and H. Berke, "Post-synthesis amine borane functionalization of a metal-organic framework and its unusual chemical hydrogen release phenomenon," Chem.—A Eur. J. **23**, 8823–8828 (2017).

[58]P. S. Petkov, V. Bon, C. L. Hobday, A. B. Kuc, P. Melix, S. Kaskel, T. Düren, and T. Heine, "Conformational isomerism controls collective flexibility in metal-organic framework DUT-8(Ni)," Phys. Chem. Chem. Phys. **21**, 674–680 (2019).

[59]A. U. Ortiz, A. Boutin, and F. X. Coudert, "Prediction of flexibility of metal–organic frameworks CAU-13 and NOTT-300 by first principles molecular simulations," Chem. Commun. **50**, 5867–5870 (2014).

[60]V. Haigis, F. X. Coudert, R. Vuilleumier, and A. Boutin, "Investigation of structure and dynamics of the hydrated metal-organic framework MIL-53(Cr) using first-principles molecular dynamics," Phys. Chem. Chem. Phys. **15**, 19049–19056 (2013).

[61]R. Demuynck, S. M. J. Rogge, L. Vanduyfhuys, J. Wieme, M. Waroquier, and V. Van Speybroeck, "Efficient construction of free energy profiles of breathing metal-organic frameworks using advanced molecular dynamics simulations," J. Chem. Theory Comput. **13**, 5861–5873 (2017).

[62]L. Chen, J. P. S. Mowat, D. Fairen-Jimenez, C. A. Morrison, S. P. Thompson, P. A. Wright, and T. Düren, "Elucidating the breathing of the metal-organic framework MIL-53(Sc) with *ab initio* molecular dynamics simulations and *in situ* x-ray powder diffraction experiments," J. Am. Chem. Soc. **135**, 15763–15773 (2013).

[63]L. Bellarosa, S. Calero, and N. López, "Early stages in the degradation of metal-organic frameworks in liquid water from first-principles molecular dynamics," Phys. Chem. Chem. Phys. **14**, 7240–7245 (2012).

[64]L. Bellarosa, J. M. Castillo, T. Vlugt, S. Calero, and N. López, "On the mechanism behind the instability of isoreticular metal-organic frameworks (IRMOFs) in humid environments," Chem.—A Eur. J. **18**, 12260–12266 (2012).

[65]V. Haigis, F. X. Coudert, R. Vuilleumier, A. Boutin, and A. H. Fuchs, "Hydrothermal breakdown of flexible metal-organic frameworks: A study by first-principles molecular dynamics," J. Phys. Chem. Lett. **6**, 4365–4370 (2015).

[66]R. Koitz, J. Hutter, and M. Iannuzzi, "Formation and properties of a terpyridine-based 2D MOF on the surface of water," 2D Mater. **3**, 025026 (2016).

[67]R. Koitz, M. Iannuzzi, and J. Hutter, "Building blocks for two-dimensional metal-organic frameworks confined at the air-water interface: An *ab initio* molecular dynamics study," J. Phys. Chem. C **119**, 4023–4030 (2015).

[68]E. Eisbein, J. O. Joswig, and G. Seifert, "Enhanced proton-transfer activity in imidazole@MIL-53(Al) systems revealed by molecular-dynamics simulations," Microporous Mesoporous Mater. **216**, 36–41 (2014).

[69]L. Pan, G. Liu, H. Li, S. Meng, L. Han, J. Shang, and B. Chen, "A resistance-switchable and ferroelectric metal−organic framework," J. Am. Chem. Soc. **136**, 17477–17483 (2014).

[70]A. A. Simagina, M. V. Polynski, A. V. Vinogradov, and E. A. Pidko, "Towards rational design of metal-organic framework-based drug delivery systems," Russ. Chem. Rev. **87**, 831–858 (2018).

[71]S. Zuluaga, P. Canepa, K. Tan, Y. J. Chabal, and T. Thonhauser, "Study of van der Waals bonding and interactions in metal organic framework materials," J. Phys. Condens. Matter **26**, 133002 (2014).

[72]S. Ehrlich, J. Moellmann, W. Reckien, T. Bredow, and S. Grimme, "System-dependent dispersion coefficients for the DFT-D3 treatment of adsorption processes on ionic surfaces," ChemPhysChem **12**, 3414–3420 (2011).

[73]J. Klimeš, D. R. Bowler, and A. Michaelides, "Van der Waals density functionals applied to solids," Phys. Rev. B **83**, 195131 (2011).

[74]M. K. Rana, H. S. Koh, J. Hwang, and D. J. Siegel, "Comparing van der Waals density functionals for CO_2 adsorption in metal organic frameworks," J. Phys. Chem. C **116**, 16957–16968 (2012).

[75]H. S. Koh, M. K. Rana, J. Hwang, and D. J. Siegel, "Thermodynamic screening of metal-substituted MOFs for carbon capture," Phys. Chem. Chem. Phys. **15**, 4573–4581 (2013).

[76]G. W. Mann, K. Lee, M. Cococcioni, B. Smit, and J. B. Neaton, "First-principles Hubbard U approach for small molecule binding in metal-organic frameworks," J. Chem. Phys. **144**, 174104 (2016).

[77]K. Lee, J. D. Howe, L. C. Lin, B. Smit, and J. B. Neaton, "Small-molecule adsorption in open-site metal-organic frameworks: A systematic density functional theory study for rational design," Chem. Mater. **27**, 668–678 (2015).

[78]H. Kim, J. Park, and Y. Jung, "The binding nature of light hydrocarbons on Fe/MOF-74 for gas separation," Phys. Chem. Chem. Phys. **15**, 19644–19650 (2013).

[79]L. Valenzano, B. Civalleri, S. Chavan, G. T. Palomino, C. O. Areán, and S. Bordiga, "Computational and experimental studies on the adsorption of CO, N_2, and CO_2 on Mg-MOF-74," J. Phys. Chem. C **114**, 11185–11191 (2010).

[80]M. Delle Piane, M. Corno, A. Pedone, R. Dovesi, and P. Ugliengo, "Large-scale B3LYP simulations of ibuprofen adsorbed in MCM-41 mesoporous silica as drug delivery system," J. Phys. Chem. C **118**, 26737–26749 (2014).

[81]P. E. Blöchl, "Projector augmented-wave method," Phys. Rev. B **50**, 17953–17979 (1994).

[82]M. D'Amore, B. Civalleri, I. J. Bush, E. Albanese, and M. Ferrabone, "Elucidating the interaction of CO_2 in the giant metal-organic framework MIL-100 through large-scale periodic *ab initio* modeling," J. Phys. Chem. C **123**, 28677–28687 (2019).

[83]W. You, Y. Liu, J. D. Howe, D. Tang, and D. S. Sholl, "Tuning binding tendencies of small molecules in metal-organic frameworks with open metal sites by metal substitution and linker functionalization," J. Phys. Chem. C **122**, 27486–27494 (2018).

[84]D. Cunha, M. Ben Yahia, S. Hall, S. R. Miller, H. Chevreau, E. Elkaïm, G. Maurin, P. Horcajada, and C. Serre, "Rationale of drug encapsulation and release from biocompatible porous metal-organic frameworks," Chem. Mater. **25**, 2767–2776 (2013).

[85]Z. Zhang, K. R. Yang, and X. Xu, "Understanding the separation mechanism of C_2H_6/C_2H_4 on zeolitic imidazolate framework ZIF-7 by periodic DFT investigations," J. Phys. Chem. C **124**, 256–266 (2020).

[86]M. Zhang, X. Huang, and Y. Chen, "DFT insights into the adsorption of NH_3-SCR related small gases in Mn-MOF-74," Phys. Chem. Chem. Phys. **18**, 28854–28863 (2016).

[87]R. Das, D. Muthukumar, R. S. Pillai, and C. M. Nagaraja, "Rational design of a Zn^{II} MOF with multiple functional sites for highly efficient fixation of CO_2 under mild conditions: Combined experimental and theoretical investigation," Chem.—A Eur. J. **26**, 17445–17454 (2020).

[88]J. Ye and J. K. Johnson, "Design of Lewis pair-functionalized metal organic frameworks for CO_2 hydrogenation," ACS Catal. **5**, 2921–2928 (2015).

[89]J. Ye and J. K. Johnson, "Catalytic hydrogenation of CO_2 to methanol in a Lewis pair functionalized MOF," Catal. Sci. Technol. **6**, 8392–8405 (2016).

[90]R. F. W. Bader, J. Hernández-Trujillo, and F. Cortés-Guzmán, "Chemical bonding: From Lewis to atoms in molecules," J. Comput. Chem. **28**, 4–14 (2007).

[91]T. Vazhappilly, T. K. Ghanty, and B. N. Jagatap, "Computational modeling of adsorption of Xe and Kr in M-MOF-74 metal organic frame works with different metal atoms," J. Phys. Chem. C **120**, 10968–10974 (2016).

[92]T. Lescouet, C. Chizallet, and D. Farrusseng, "The origin of the activity of amine-functionalized metal-organic frameworks in the catalytic synthesis of cyclic carbonates from epoxide and CO_2," ChemCatChem **4**, 1725–1728 (2012).

[93]P. Canepa, C. A. Arter, E. M. Conwill, D. H. Johnson, B. A. Shoemaker, K. Z. Soliman, and T. Thonhauser, "High-throughput screening of small-molecule adsorption in MOF," J. Mater. Chem. A **1**, 13597–13604 (2013).

[94]S. Jensen, K. Tan, W. Lustig, D. Kilin, J. Li, Y. J. Chabal, and T. Thonhauser, "Quenching of photoluminescence in a Zn-MOF sensor by nitroaromatic molecules," J. Mater. Chem. C **7**, 2625–2632 (2019).

[95]P. Horcajada, C. Serre, G. Maurin, N. A. Ramsahye, F. Balas, M. Vallet-Regí, M. Sebban, F. Taulelle, and G. Férey, "Flexible porous metal-organic frameworks for a controlled drug delivery," J. Am. Chem. Soc. **130**, 6774–6780 (2008).

[96]S. Devautour-Vinot, C. Martineau, S. Diaby, M. Ben-Yahia, S. Miller, C. Serre, P. Horcajada, D. Cunha, F. Taulelle, and G. Maurin, "Caffeine confinement into a series of functionalized porous zirconium MOFs: A joint experimental/modeling exploration," J. Phys. Chem. C **117**, 11694–11704 (2013).

[97]C. Vieira Soares, G. Maurin, and A. A. Leitaõ, "Computational exploration of the catalytic degradation of sarin and its simulants by a titanium metal-organic framework," J. Phys. Chem. C **123**, 19077–19086 (2019).

07 May 2024 15:47:34

[98] D. N. Dybtsev, M. P. Yutkin, D. G. Samsonenko, V. P. Fedin, A. L. Nuzhdin, A. A. Bezrukov, K. P. Bryliakov, E. P. Talsi, R. V. Belosludov, H. Mizuseki, Y. Kawazoe, O. S. Subbotin, and V. R. Belosludov, "Modular, homochiral, porous coordination polymers: Rational design, enantioselective guest exchange sorption and *ab initio* calculations of host-guest interactions," Chem.—A Eur. J. **16**, 10348–10356 (2010).

[99] D. Yan, Y. Tang, H. Lin, and D. Wang, "Tunable two-color luminescence and host-guest energy transfer of fluorescent chromophores encapsulated in metal-organic frameworks," Sci. Rep. **4**, 4337 (2014).

[100] M. D. Allendorf, M. E. Foster, F. Léonard, V. Stavila, P. L. Feng, F. P. Doty, K. Leong, E. Y. Ma, S. R. Johnston, and A. A. Talin, "Guest-induced emergent properties in metal-organic frameworks," J. Phys. Chem. Lett. **6**, 1182–1195 (2015).

[101] K. Lee, W. C. Isley, A. L. Dzubak, P. Verma, S. J. Stoneburner, L. C. Lin, J. D. Howe, E. D. Bloch, D. A. Reed, M. R. Hudson, C. M. Brown, J. R. Long, J. B. Neaton, B. Smit, C. J. Cramer, D. G. Truhlar, and L. Gagliardi, "Design of a metal-organic framework with enhanced back bonding for separation of N_2 and CH_4," J. Am. Chem. Soc. **136**, 698–704 (2014).

[102] B. Supronowicz, A. Mavrandonakis, and T. Heine, "Interaction of small gases with the unsaturated metal centers of the HKUST-1 metal organic framework," J. Phys. Chem. C **117**, 14570–14578 (2013).

[103] E. N. Koukaras, A. D. Zdetsis, and G. E. Froudakis, "Theoretical study of amino acid interaction with metal organic frameworks," J. Phys. Chem. Lett. **2**, 272–275 (2011).

[104] S. J. Stoneburner and L. Gagliardi, "Air separation by catechol-ligated transition metals: A quantum chemical screening," J. Phys. Chem. C **122**, 22345–22351 (2018).

[105] S. J. Stoneburner, V. Livermore, M. E. McGreal, D. Yu, K. D. Vogiatzis, R. Q. Snurr, and L. Gagliardi, "Catechol-ligated transition metals: A quantum chemical study on a promising system for gas separation," J. Phys. Chem. C **121**, 10463–10469 (2017).

[106] V. Bernales, A. B. League, Z. Li, N. M. Schweitzer, A. W. Peters, R. K. Carlson, J. T. Hupp, C. J. Cramer, O. K. Farha, and L. Gagliardi, "Computationally guided discovery of a catalytic cobalt-decorated metal-organic framework for ethylene dimerization," J. Phys. Chem. C **120**, 23576–23583 (2016).

[107] M. Kotzabasaki, E. Tylianakis, E. Klontzas, and G. E. Froudakis, "OH-functionalization strategy in metal-organic frameworks for drug delivery," Chem. Phys. Lett. **685**, 114–118 (2017).

[108] J. Pirillo and Y. Hijikata, "Trans influence across a metal–metal bond of a paddle-wheel unit on interaction with gases in a metal-organic framework," Inorg. Chem. **59**, 1193–1203 (2020).

[109] D. E. Ortega, "Theoretical insight into the effect of fluorine-functionalized metal-organic framework supported palladium single-site catalyst in the ethylene dimerization reaction," Chem.—A Eur. J. **27**, 10413–10421 (2021).

[110] B. Supronowicz, A. Mavrandonakis, and T. Heine, "Interaction of biologically important organic molecules with the unsaturated copper centers of the HKUST-1 metal-organic framework: An *ab-initio* study," J. Phys. Chem. C **119**, 3024–3032 (2015).

[111] M. Ernst and G. Gryn'ova, "Strength and nature of host-guest interactions in metal-organic frameworks from a quantum-chemical perspective," ChemPhysChem **23**, e202200098 (2022).

[112] B. Jeziorski, R. Moszynski, and K. Szalewicz, "Perturbation theory approach to intermolecular potential energy surfaces of van der Waals complexes," Chem. Rev. **94**, 1887–1930 (1994).

[113] D. Yang, S. O. Odoh, T. C. Wang, O. K. Farha, J. T. Hupp, C. J. Cramer, L. Gagliardi, and B. C. Gates, "Metal-organic framework nodes as nearly ideal supports for molecular catalysts: NU-1000- and UiO-66-supported iridium complexes," J. Am. Chem. Soc. **137**, 7391–7396 (2015).

[114] Z. Li, A. W. Peters, V. Bernales, M. A. Ortuño, N. M. Schweitzer, M. R. Destefano, L. C. Gallington, A. E. Platero-Prats, K. W. Chapman, C. J. Cramer, L. Gagliardi, J. T. Hupp, and O. K. Farha, "Metal-organic framework supported cobalt catalysts for the oxidative dehydrogenation of propane at low temperature," ACS Cent. Sci. **3**, 31–38 (2017).

[115] T. Maihom, M. Probst, and J. Limtrakul, "Computational study of the carbonylene reaction between formaldehyde and propylene encapsulated in coordinatively unsaturated metal-organic frameworks $M_3(btc)_2$ (M = Fe, Co, Ni, Cu, and Zn)," Phys. Chem. Chem. Phys. **21**, 2783–2789 (2019).

[116] H. Chen, P. Liao, M. L. Mendonca, and R. Q. Snurr, "Insights into catalytic hydrolysis of organophosphate warfare agents by metal-organic framework NU-1000," J. Phys. Chem. C **122**, 12362–12368 (2018).

[117] T. Islamoglu, M. A. Ortuño, E. Proussaloglou, A. J. Howarth, N. A. Vermeulen, A. Atilgan, A. M. Asiri, C. J. Cramer, and O. K. Farha, "Presence versus proximity: The role of pendant amines in the catalytic hydrolysis of a nerve agent simulant," Angew. Chem. - Int. Ed. **57**, 1949–1953 (2018).

[118] J. G. Vitillo, A. Bhan, C. J. Cramer, C. C. Lu, and L. Gagliardi, "Quantum chemical characterization of structural single Fe(II) sites in MIL-type metal-organic frameworks for the oxidation of methane to methanol and ethane to ethanol," ACS Catal. **9**, 2870–2879 (2019).

[119] Y. Hidalgo-Rosa, M. A. Treto-Suárez, E. Schott, X. Zarate, and D. Páez-Hernández, "Sensing mechanism elucidation of a europium(III) metal–organic framework selective to aniline: A theoretical insight by means of multiconfigurational calculations," J. Comput. Chem. **41**, 1956–1964 (2020).

[120] Y. Hidalgo-Rosa, K. Mena-Ulecia, M. A. Treto-Suárez, E. Schott, D. Páez-Hernández, and X. Zarate, "Insights into the selective sensing mechanism of a luminescent Cd(II)-based MOF chemosensor toward NACs: Roles of the host–guest interactions and PET processes," J. Mater. Sci. **56**, 13684–13704 (2021).

[121] Y. Yao, X. Song, J. Qiu, and C. Hao, "Interaction between formaldehyde and luminescent MOF $[Zn(NH_2bdc)(bix)]_n$ in the electronic excited state," J. Phys. Chem. A **118**, 6191–6196 (2014).

[122] M. Dixit, T. A. Maark, and S. Pal, "*Ab initio* and periodic DFT investigation of hydrogen storage on light metal-decorated MOF-5," Int. J. Hydrogen Energy. **36**, 10816–10827 (2011).

[123] L. Valenzano, B. Civalleri, K. Sillar, and J. Sauer, "Heats of adsorption of CO and CO_2 in metal-organic frameworks: Quantum mechanical study of CPO-27-M (M = Mg, Ni, Zn)," J. Phys. Chem. C **115**, 21777–21784 (2011).

[124] A. Kundu, G. Piccini, K. Sillar, and J. Sauer, "*Ab initio* prediction of adsorption isotherms for small molecules in metal-organic frameworks," J. Am. Chem. Soc. **138**, 14047–14056 (2016).

[125] M. Rubes, A. D. Wiersum, P. L. Llewellyn, L. Grajciar, O. Bludský, and P. Nachtigall, "Adsorption of propane and propylene on CuBTC metal-organic framework: Combined theoretical and experimental investigation," J. Phys. Chem. C **117**, 11159–11167 (2013).

[126] L. Grajciar, O. Bludský, and P. Nachtigall, "Water adsorption on coordinatively unsaturated sites in CuBTC MOF," J. Phys. Chem. Lett. **1**, 3354–3359 (2010).

[127] L. Grajciar, A. D. Wiersum, P. L. Llewellyn, J. S. Chang, and P. Nachtigall, "Understanding CO_2 adsorption in CuBTC MOF: Comparing combined DFT-*ab initio* calculations with microcalorimetry experiments," J. Phys. Chem. C **115**, 17925–17933 (2011).

[128] D. Yu, A. O. Yazaydin, J. R. Lane, P. D. C. Dietzel, and R. Q. Snurr, "A combined experimental and quantum chemical study of CO_2 adsorption in the metal–organic framework CPO-27 with different metals," Chem. Sci. **4**, 3544 (2013).

[129] I. Casademont-Reig, T. Woller, J. Contreras-García, M. Alonso, M. Torrent-Sucarrat, and E. Matito, "New electron delocalization tools to describe the aromaticity in porphyrinoids," Phys. Chem. Chem. Phys. **20**, 2787–2796 (2018).

[130] I. Fernández and G. Frenking, "The Diels–Alder reaction from the EDA-NOCV perspective: A re-examination of the frontier molecular orbital model," Eur. J. Org. Chem. **2019**, 478–485.

[131] M. J. S. Phipps, T. Fox, C. S. Tautermann, and C. K. Skylaris, "Energy decomposition analysis approaches and their evaluation on prototypical protein-drug interaction patterns," Chem. Soc. Rev. **44**, 3177–3211 (2015).

[132] D. Arias-Olivares, E. K. Wieduwilt, J. Contreras-García, and A. Genoni, "NCI-ELMO: A new method to quickly and accurately detect noncovalent interactions in biosystems," J. Chem. Theory Comput. **15**, 6456–6470 (2019).

[133] B. Meyer, S. Barthel, A. Mace, L. Vannay, B. Guillot, B. Smit, and C. Corminboeuf, "DORI reveals the influence of noncovalent interactions on covalent bonding patterns in molecular crystals under pressure," J. Phys. Chem. Lett. **10**, 1482–1488 (2019).

[134] N. Casati, A. Kleppe, A. P. Jephcoat, and P. Macchi, "Putting pressure on aromaticity along with *in situ* experimental electron density of a molecular crystal," Nat. Commun. **7**, 10901 (2016).

[135]E. Tsivion, J. R. Long, and M. Head-Gordon, "Hydrogen physisorption on metal-organic framework linkers and metalated linkers: A computational study of the factors that control binding strength," J. Am. Chem. Soc. **136**, 17827–17835 (2014).

[136]D. E. Jaramillo, H. Z. H. Jiang, H. A. Evans, R. Chakraborty, H. Furukawa, C. M. Brown, M. Head-Gordon, and J. R. Long, "Ambient-temperature hydrogen storage via vanadium(II)-dihydrogen complexation in a metal-organic framework," J. Am. Chem. Soc. **143**, 6248–6256 (2021).

[137]M. M. Deshmukh and S. Sakaki, "Binding energy of gas molecule with two pyrazine molecules as organic linker in metal-organic framework: Its theoretical evaluation and understanding of determining factors," Theor. Chem. Acc. **130**, 475–482 (2011).

[138]Y. Hidalgo-Rosa, M. A. Treto-Suárez, E. Schott, X. Zarate, and D. Páez-Hernández, "Sensing mechanism elucidation of a chemosensor based on a metal-organic framework selective to explosive aromatic compounds," Int. J. Quantum Chem. **120**, e26404 (2020).

[139]J. J. Goings, S. M. Ohlsen, K. M. Blaisdell, and D. P. Schofield, "Sorption of H_2 to open metal sites in a metal–organic framework: A symmetry-adapted perturbation theory analysis," J. Phys. Chem. A **118**, 7411–7417 (2014).

[140]X. L. Xiong, G. H. Chen, S. T. Xiao, Y. G. Ouyang, H. B. Li, and Q. Wang, "New discovery of metal-organic framework utsa-280: Ultrahigh adsorption selectivity of krypton over xenon," J. Phys. Chem. C **124**, 14603–14612 (2020).

[141]E. N. Koukaras, T. Montagnon, P. Trikalitis, D. Bikiaris, A. D. Zdetsis, and G. E. Froudakis, "Toward efficient drug delivery through suitably prepared metal-organic frameworks: A first-principles study," J. Phys. Chem. C **118**, 8885–8890 (2014).

[142]H. Tan, Q. Chen, Y. Sheng, X. Li, and H. Liu, "Guest-induced reversible crystal-to-amorphous-to-crystal transformation in a Co(II)-based metal–organic framework," CrystEngComm. **20**, 6828–6833 (2018).

[143]T. Loiseau, C. Serre, C. Huguenard, G. Fink, F. Taulelle, M. Henry, T. Bataille, and G. Férey, "A rationale for the large breathing of the porous aluminum terephthalate (MIL-53) upon hydration," Chem.—A Eur. J. **10**, 1373–1382 (2004).

[144]C. Serre, F. Millange, C. Thouvenot, M. Noguès, G. Marsolier, D. Louër, and G. Férey, "Very large breathing effect in the first nanoporous chromium(III)-based solids: MIL-53 or $Cr^{III}(OH)\cdot\{O_2C\text{-}C_6H_4\text{-}CO_2\}\cdot\{HO_2C\text{-}C_6H\text{-}CO_2H\}_x\cdot H_2O_y$," J. Am. Chem. Soc. **124**, 13519–13526 (2002).

[145]Q. Ma, Q. Yang, A. Ghoufi, K. Yang, M. Lei, G. Férey, C. Zhong, and G. Maurin, "Guest-modulation of the mechanical properties of flexible porous metal-organic frameworks," J. Mater. Chem. A **2**, 9691–9698 (2014).

[146]H. C. Dong, H. L. Nguyen, H. M. Le, N. Thoai, Y. Kawazoe, and D. Nguyen-Manh, "Monitoring mechanical, electronic, and catalytic trends in a titanium metal organic framework under the influence of guest-molecule encapsulation using density functional theory," Sci. Rep. **8**, 16651 (2018).

[147]P. Canepa, K. Tan, Y. Du, H. Lu, Y. J. Chabal, and T. Thonhauser, "Structural, elastic, thermal, and electronic responses of small-molecule-loaded metal-organic framework materials," J. Mater. Chem. A **3**, 986–995 (2015).

[148]R. Scatena, Y. T. Guntern, and P. Macchi, "Electron density and dielectric properties of highly porous MOFs: Binding and mobility of guest molecules in $Cu_3(BTC)_2$ and $Zn_3(BTC)_2$," J. Am. Chem. Soc. **141**, 9382–9390 (2019).

[149]A. A. Talin, A. Centrone, A. C. Ford, M. E. Foster, V. Stavila, P. Haney, R. A. Kinney, V. Szalai, F. El Gabaly, H. P. Yoon, F. Léonard, and M. D. Allendorf, "Tunable electrical conductivity in metal-organic framework thin-film devices," Science **343**, 66–69 (2014).

[150]D. Aravena, Z. A. Castillo, M. C. Muñoz, A. B. Gaspar, K. Yoneda, R. Ohtani, A. Mishima, S. Kitagawa, M. Ohba, J. A. Real, and E. Ruiz, "Guest modulation of spin-crossover transition temperature in a porous iron(II) metal-organic framework: Experimental and periodic DFT studies," Chem.—A Eur. J. **20**, 12864–12873 (2014).

[151]X. Yang and D. Yan, "Long-afterglow metal-organic frameworks: Reversible guest-induced phosphorescence tunability," Chem. Sci. **7**, 4519–4526 (2016).

[152]Y. G. Chung, J. Camp, M. Haranczyk, B. J. Sikora, W. Bury, V. Krungleviciute, T. Yildirim, O. K. Farha, D. S. Sholl, and R. Q. Snurr, "Computation-ready, experimental metal–organic frameworks: A tool to enable high-throughput screening of nanoporous crystals," Chem. Mater. **26**, 6185–6192 (2014).

[153]Y. J. Colón and R. Q. Snurr, "High-throughput computational screening of metal-organic frameworks," Chem. Soc. Rev. **43**, 5735–5749 (2014).

[154]A. Sturluson, M. T. Huynh, A. R. Kaija, C. Laird, S. Yoon, F. Hou, Z. Feng, C. E. Wilmer, Y. J. Colón, Y. G. Chung, D. W. Siderius, and C. M. Simon, "The role of molecular modelling and simulation in the discovery and deployment of metal-organic frameworks for gas storage and separation," Mol. Simul. **45**, 1082–1121 (2019).

[155]C. E. Wilmer, M. Leaf, C. Y. Lee, O. K. Farha, B. G. Hauser, J. T. Hupp, and R. Q. Snurr, "Large-scale screening of hypothetical metal–organic frameworks," Nat. Chem. **4**, 83–89 (2012).

[156]B. J. Sikora, C. E. Wilmer, M. L. Greenfield, and R. Q. Snurr, "Thermodynamic analysis of Xe/Kr selectivity in over 137000 hypothetical metal-organic frameworks," Chem. Sci. **3**, 2217–2223 (2012).

[157]C. E. Wilmer, O. K. Farha, Y. S. Bae, J. T. Hupp, and R. Q. Snurr, "Structure-property relationships of porous materials for carbon dioxide separation and capture," Energy Environ. Sci. **5**, 9849–9856 (2012).

[158]N. S. Bobbitt, J. Chen, and R. Q. Snurr, "High-throughput screening of metal-organic frameworks for hydrogen storage at cryogenic temperature," J. Phys. Chem. C **120**, 27328–27341 (2016).

[159]S. Li, Y. G. Chung, and R. Q. Snurr, "High-throughput screening of metal-organic frameworks for CO_2 capture in the presence of water," Langmuir **32**, 10368–10376 (2016).

[160]J. Rogacka, A. Seremak, A. Luna-Triguero, F. Formalik, I. Matito-Martos, L. Firlej, S. Calero, and B. Kuchta, "High-throughput screening of metal–organic frameworks for CO_2 and CH_4 separation in the presence of water," Chem. Eng. J. **403**, 126392 (2021).

[161]V. A. Solanki and B. Borah, "High-throughput computational screening of 12,351 real metal-organic framework structures for separation of hexane isomers: A quest for a yet better adsorbent," J. Phys. Chem. C **124**, 4582–4594 (2020).

[162]C. Altintas, I. Erucar, and S. Keskin, "High-throughput computational screening of the metal organic framework database for CH_4/H_2 separations," ACS Appl. Mater. Interfaces **10**, 3668–3679 (2018).

[163]H. Demir, S. J. Stoneburner, W. Jeong, D. Ray, X. Zhang, O. K. Farha, C. J. Cramer, J. I. Siepmann, and L. Gagliardi, "Metal-organic frameworks with metal-catecholates for O_2/N_2 separation," J. Phys. Chem. C **123**, 12935–12946 (2019).

[164]Y. Pramudya, S. Bonakala, D. Antypov, P. M. Bhatt, A. Shkurenko, M. Eddaoudi, M. J. Rosseinsky, and M. S. Dyer, "High-throughput screening of metal-organic frameworks for kinetic separation of propane and propene," Phys. Chem. Chem. Phys. **22**, 23073–23082 (2020).

[165]C. Gu, Z. Yu, J. Liu, and D. S. Sholl, "Construction of an anion-pillared MOF database and the screening of MOFs suitable for Xe/Kr separation," ACS Appl. Mater. Interfaces **13**, 11039–11049 (2021).

[166]A. S. Rosen, J. M. Notestein, and R. Q. Snurr, "Identifying promising metal–organic frameworks for heterogeneous catalysis via high-throughput periodic density functional theory," J. Comput. Chem. **40**, 1305–1318 (2019).

[167]A. S. Rosen, J. M. Notestein, and R. Q. Snurr, "Structure-activity relationships that identify metal-organic framework catalysts for methane activation," ACS Catal. **9**, 3576–3587 (2019).

[168]A. S. Rosen, M. R. Mian, T. Islamoglu, H. Chen, O. K. Farha, J. M. Notestein, and R. Q. Snurr, "Tuning the redox activity of metal-organic frameworks for enhanced, selective O_2 binding: Design rules and ambient temperature O_2 chemisorption in a cobalt-triazolate framework," J. Am. Chem. Soc. **142**, 4317–4328 (2020).

[169]N. E. R. Zimmermann and A. Jain, "Local structure order parameters and site fingerprints for quantification of coordination environment and crystal structure similarity," RSC Adv. **10**, 6063–6081 (2020).

[170]M. Fumanal, G. Capano, S. Barthel, B. Smit, and I. Tavernelli, "Energy-based descriptors for photo-catalytically active metal-organic framework discovery," J. Mater. Chem. A **8**, 4473–4482 (2020).

[171]E. L. First, C. E. Gounaris, and C. A. Floudas, "Predictive framework for shape-selective separations in three-dimensional zeolites and metal-organic frameworks," Langmuir **29**, 5599–5608 (2013).

[172]E. L. First and C. A. Floudas, "MOFomics: Computational pore characterization of metal–organic frameworks," Microporous Mesoporous Mater. **165**, 32–39 (2013).

07 May 2024 15:47:34

[173]P. Z. Moghadam, T. Islamoglu, S. Goswami, J. Exley, M. Fantham, C. F. Kaminski, R. Q. Snurr, O. K. Farha, and D. Fairen-Jimenez, "Computer-aided discovery of a metal-organic framework with superior oxygen uptake," Nat. Commun. **9**, 1387 (2018).

[174]N. S. Bobbitt and R. Q. Snurr, "Molecular modelling and machine learning for high-throughput screening of metal-organic frameworks for hydrogen storage," Mol. Simul. **45**, 1069–1081 (2019).

[175]Z. Shi, W. Yang, X. Deng, C. Cai, Y. Yan, H. Liang, Z. Liu, and Z. Qiao, "Machine-learning-assisted high-throughput computational screening of high performance metal-organic frameworks," Mol. Syst. Des. Eng. **5**, 725–742 (2020).

[176]C. Altintas, O. F. Altundal, S. Keskin, and R. Yildirim, "Machine learning meets with metal organic frameworks for gas storage and separation," J. Chem. Inf. Model. **61**, 2131–2146 (2021).

[177]K. M. Jablonka, D. Ongari, S. M. Moosavi, and B. Smit, "Big-data science in porous materials: Materials genomics and machine learning," Chem. Rev. **120**, 8066–8129 (2020).

[178]S. Chong, S. Lee, B. Kim, and J. Kim, "Applications of machine learning in metal-organic frameworks," Coord. Chem. Rev. **423**, 213487 (2020).

[179]H. Demir, H. Daglar, H. C. Gulbalkan, G. O. Aksu, and S. Keskin, "Recent advances in computational modeling of MOFs: From molecular simulations to machine learning," Coord. Chem. Rev. **484**, 215112 (2023).

[180]A. S. Rosen, S. M. Iyer, D. Ray, Z. Yao, A. Aspuru-Guzik, L. Gagliardi, J. M. Notestein, and R. Q. Snurr, "Machine learning the quantum-chemical properties of metal–organic frameworks for accelerated materials discovery," Matter **4**, 1578–1597 (2021).

[181]M. Fernandez, N. R. Tre, and T. K. Woo, "Atomic property weighted radial distribution functions descriptors of metal–organic frameworks for the prediction of gas uptake capacity," J. Phys. Chem. C **117**, 14095–14105 (2013).

[182]M. Fernandez, T. K. Woo, C. E. Wilmer, and R. Q. Snurr, "Large-scale quantitative structure-property relationship (QSPR) analysis of methane storage in metal-organic frameworks," J. Phys. Chem. C **117**, 7681–7689 (2013).

[183]P. Halder and J. K. Singh, "High-throughput screening of metal–organic frameworks for ethane–ethylene separation using the machine learning technique," Energy Fuels **34**, 14591–14597 (2020).

[184]W. Yang, H. Liang, F. Peng, Z. Liu, J. Liu, and Z. Qiao, "Computational screening of metal-organic framework membranes for the separation of 15 gas mixtures," Nanomaterials **9**, 467 (2019).

[185]Z. Qiao, Y. Yan, Y. Tang, H. Liang, and J. Jiang, "Metal–organic frameworks for xylene separation: From computational screening to machine learning," J. Phys. Chem. C **125**, 7839–7848 (2021).

[186]M. Fernandez, P. G. Boyd, T. D. Daff, M. Z. Aghaji, and T. K. Woo, "Rapid and accurate machine learning recognition of high performing metal organic frameworks for CO_2 capture," J. Phys. Chem. Lett. **5**, 3056–3060 (2014).

[187]H. Dureckova, M. Krykunov, M. Z. Aghaji, and T. K. Woo, "Robust machine learning models for predicting high CO_2 working capacity and CO_2/H_2 selectivity of gas adsorption in metal organic frameworks for precombustion carbon capture," J. Phys. Chem. C **123**, 4133–4139 (2019).

[188]M. Pardakhti, E. Moharreri, D. Wanik, S. L. Suib, and R. Srivastava, "Machine learning using combined structural and chemical descriptors for prediction of methane adsorption performance of metal organic frameworks (MOFs)," ACS Comb. Sci. **19**, 640–645 (2017).

[189]G. S. Fanourgakis, K. Gkagkas, E. Tylianakis, and G. E. Froudakis, "A universal machine learning algorithm for large-scale screening of materials," J. Am. Chem. Soc. **142**, 3814–3822 (2020).

[190]M. Rupp, O. A. Von Lilienfeld, and K. Burke, "Guest editorial: Special topic on data-enabled theoretical chemistry," J. Chem. Phys. **148**, 241401 (2018).

[191]X. Wu, S. Xiang, J. Su, and W. Cai, "Understanding quantitative relationship between methane storage capacities and characteristic properties of metal-organic frameworks based on machine learning," J. Phys. Chem. C **123**, 8550–8559 (2019).

[192]S. Li, Y. Zhang, Y. Hu, B. Wang, S. Sun, X. Yang, and H. He, "Predicting metal-organic frameworks as catalysts to fix carbon dioxide to cyclic carbonate by machine learning," J. Materiomics **7**, 1029–1038 (2021).

[193]H. Liang, W. Yang, F. Peng, Z. Liu, J. Liu, and Z. Qiao, "Combining large-scale screening and machine learning to predict the metal-organic frameworks for organosulfurs removal from high-sour natural gas," APL Mater. **7**, 091101 (2019).

[194]I. Tsamardinos, G. S. Fanourgakis, E. Greasidou, E. Klontzas, K. Gkagkas, and G. E. Froudakis, "An automated machine learning architecture for the accelerated prediction of metal-organic frameworks performance in energy and environmental applications," Microporous Mesoporous Mater. **300**, 110160 (2020).

[195]S. Vandenhaute, M. Cools-Ceuppens, S. DeKeyser, T. Verstraelen, and V. Van Speybroeck, "Machine learning potentials for metal-organic frameworks using an incremental learning approach," npj Comput. Mater. **9**, 19 (2023).

[196]R. Wang, Y. Zhong, L. Bi, M. Yang, and D. Xu, "Accelerating discovery of metal-organic frameworks for methane adsorption with hierarchical screening and deep learning," ACS Appl. Mater. Interfaces **12**, 52797–52807 (2020).

[197]X. Zhang, K. Zhang, H. Yoo, and Y. Lee, "Machine learning-driven discovery of metal-organic frameworks for efficient CO_2 capture in humid condition," ACS Sustainable Chem. Eng. **9**, 2872–2879 (2021).

[198]X. Sun, W. Lin, K. Jiang, H. Liang, and G. Chen, "Accelerated screening and assembly of promising MOFs with open Cu sites for isobutene/isobutane separation using a data-driven approach," Phys. Chem. Chem. Phys. **25**, 8608–8623 (2023).

[199]A. Kuc, M. A. Springer, K. Batra, R. Juarez-Mosqueda, C. Wöll, and T. Heine, "Proximity effect in crystalline framework materials: Stacking-induced functionality in MOFs and COFs," Adv. Funct. Mater. **30**, 1908004 (2020).

[200]A. Mähringer and D. D. Medina, "Taking stock of stacking," Nat. Chem. **12**, 985–987 (2020).

[201]A. M. Pütz, M. W. Terban, S. Bette, F. Haase, R. E. Dinnebier, and B. V. Lotsch, "Total scattering reveals the hidden stacking disorder in a 2D covalent organic framework," Chem. Sci. **11**, 12647–12654 (2020).

[202]E. Tylianakis, E. Klontzas, and G. E. Froudakis, "Multi-scale theoretical investigation of hydrogen storage in covalent organic frameworks," Nanoscale **3**, 856–869 (2011).

[203]H. Zhong, J. Gao, R. Sa, S. Yang, Z. Wu, and R. Wang, "Carbon dioxide conversion upgraded by host-guest cooperation between nitrogen-rich covalent organic framework and imidazolium-based ionic polymer," ChemSusChem **13**, 6323–6329 (2020).

[204]B. Dash, "Carbon dioxide capture using covalent organic frameworks (COFs) type material—a theoretical investigation," J. Mol. Model. **24**, 120 (2018).

[205]H. Hashemzadeh and H. Raissi, "Covalent organic framework as smart and high efficient carrier for anticancer drug delivery: A DFT calculations and molecular dynamics simulation study," J. Phys. D: Appl. Phys. **51**, 345401 (2018).

[206]V. S. Vyas, M. Vishwakarma, I. Moudrakovski, F. Haase, G. Savasci, C. Ochsenfeld, J. P. Spatz, and B. V. Lotsch, "Exploiting noncovalent interactions in an imine-based covalent organic framework for quercetin delivery," Adv. Mater. **28**, 8749–8754 (2016).

[207]D. Wei, J. Li, Z. Chen, L. Liang, J. Ma, M. Wei, Y. Ai, and X. Wang, "Understanding bisphenol-A adsorption in magnetic modified covalent organic frameworks: Experiments coupled with DFT calculations," J. Mol. Liq. **301**, 112431 (2020).

[208]M. Tong, Q. Yang, Q. Ma, D. Liu, and C. Zhong, "Few-layered ultrathin covalent organic framework membranes for gas separation: A computational study," J. Mater. Chem. A **4**, 124–131 (2015).

[209]Y. Wang, J. Lan, X. Yang, S. Zhong, L. Yuan, J. Li, J. Peng, Z. Chai, J. K. Gibson, M. Zhai, and W. Shi, "Superhydrophobic phosphonium modified robust 3D covalent organic framework for preferential trapping of charge dispersed oxoanionic pollutants," Adv. Funct. Mater. **32**, 2205222 (2022).

[210]H. Zhao, Y. Guan, H. Guo, R. Du, and C. Yan, "Hydrogen storage capacity on Li-decorated covalent organic framework-1: A first-principles study," Mater. Res. Express **7**, 035506 (2020).

[211]P. Srepusharawoot, E. Swatsitang, V. Amornkitbamrung, U. Pinsook, and R. Ahuja, "Hydrogen adsorption of Li functionalized covalent organic framework-366: An *ab initio* study," Int. J. Hydrogen Energy **38**, 14276–14280 (2013).

[212]P. Srepusharawoot, R. H. Scheicher, C. Moysés Araújo, A. Blomqvist, U. Pinsook, and R. Ahuja, "*Ab initio* study of molecular hydrogen adsorption in covalent organic framework-1," J. Phys. Chem. C **113**, 8498–8504 (2009).

07 May 2024 15:47:34

[213]P. Das and S. K. Mandal, "In-depth experimental and computational investigations for remarkable gas/vapor sorption, selectivity, and affinity by a porous nitrogen-rich covalent organic framework," Chem. Mater. **31**, 1584–1596 (2019).

[214]W. Chen, M. Li, W. L. Peng, L. Huang, C. Zhao, D. Acharya, W. Liu, and A. Zheng, "Covalent organic framework shows high isobutene adsorption selectivity from C4 hydrocarbons: Mechanism of interpenetration isomerism and pedal motion," Green Energy Environ. **7**, 296–306 (2021).

[215]D. Wei, A. Zhang, Y. Ai, and X. Wang, "Adsorption properties of hydrated Cr^{3+} Ions on Schiff-base covalent organic frameworks: A DFT study," Chem.—Asian J. **15**, 1140–1146 (2020).

[216]M. Tong, Y. Lan, Q. Yang, and C. Zhong, "Exploring the structure-property relationships of covalent organic frameworks for noble gas separations," Chem. Eng. Sci. **168**, 456–464 (2017).

[217]M. Tong, Y. Lan, Z. Qin, and C. Zhong, "Computation-ready, experimental covalent organic framework for methane delivery: Screening and material design," J. Phys. Chem. C **122**, 13009–13016 (2018).

[218]G. O. Aksu, H. Daglar, C. Altintas, and S. Keskin, "Computational selection of high-performing covalent organic frameworks for adsorption and membrane-based CO_2/H_2 separation," J. Phys. Chem. C **124**, 22577–22590 (2020).

[219]O. F. Altundal, C. Altintas, and S. Keskin, "Can COFs replace MOFs in flue gas separation? high-throughput computational screening of COFs for CO_2/N_2 separation," J. Mater. Chem. A **8**, 14609–14623 (2020).

[220]D. Ongari, A. V. Yakutovich, L. Talirz, and B. Smit, "Building a consistent and reproducible database for adsorption evaluation in covalent-organic frameworks," ACS Cent. Sci. **5**, 1663–1675 (2019).

[221]G. Pizzi, A. Cepellotti, R. Sabatini, N. Marzari, and B. Kozinsky, "AiiDA: Automated interactive infrastructure and database for computational science," Comput. Mater. Sci. **111**, 218–230 (2016).

[222]R. Mercado, R. S. Fu, A. V. Yakutovich, L. Talirz, M. Haranczyk, and B. Smit, "In silico design of 2D and 3D covalent organic frameworks for methane storage applications," Chem. Mater. **30**, 5069–5086 (2018).

[223]K. S. Deeg, D. Damasceno Borges, D. Ongari, N. Rampal, L. Talirz, A. V. Yakutovich, J. M. Huck, and B. Smit, "In silico discovery of covalent organic frameworks for carbon capture," ACS Appl. Mater. Interfaces **12**, 21559–21568 (2020).

[224]Y. Lan, X. Han, M. Tong, H. Huang, Q. Yang, D. Liu, X. Zhao, and C. Zhong, "Materials genomics methods for high-throughput construction of COFs and targeted synthesis," Nat. Commun. **9**, 2574 (2018).

[225]J. S. De Vos, S. Borgmans, P. Van Der Voort, S. M. J. Rogge, and V. Van Speybroeck, "ReDD-COFFEE: A ready-to-use database of covalent organic framework structures and accurate force fields to enable high-throughput screenings," J. Mater. Chem. A **11**, 7468–7487 (2023).

[226]M. Raupach and R. Tonner, "A periodic energy decomposition analysis method for the investigation of chemical bonding in extended systems," J. Chem. Phys. **142**, 194105 (2015).

[227]A. D. D. Wonanke and M. A. Addicoat, "Effect of unwanted guest molecules on the stacking configuration of covalent organic frameworks: A periodic energy decomposition analysis," Phys. Chem. Chem. Phys. **24**, 15494–15501 (2022).

[228]D. Menéndez Crespo, F. R. Wagner, E. Francisco, Á. Martín Pendás, Y. Grin, and M. Kohout, "Interacting quantum atoms method for crystalline solids," J. Phys. Chem. A **125**, 9011–9025 (2021).

[229]C. Gatti, V. R. Saunders, and C. Roetti, "Crystal field effects on the topological properties of the electron density in molecular crystals: The case of urea," J. Chem. Phys. **101**, 10686–10696 (1994).

[230]J. George, G. Petretto, A. Naik, M. Esters, A. J. Jackson, R. Nelson, R. Dronskowski, G. Rignanese, and G. Hautier, "Automated bonding analysis with crystal orbital Hamilton populations," ChemPlusChem **87**, e202200123 (2022).

[231]M. Witman, S. Ling, S. Anderson, L. Tong, K. C. Stylianou, B. Slater, B. Smit, and M. Haranczyk, "In silico design and screening of hypothetical MOF-74 analogs and their experimental synthesis," Chem. Sci. **7**, 6263–6272 (2016).

[232]R. Anderson and D. A. Gómez-Gualdrón, "Large-scale free energy calculations on a computational metal-organic frameworks database: Toward synthetic likelihood predictions," Chem. Mater. **32**, 8106–8119 (2020).

[233]A. Nandy, G. Terrones, N. Arunachalam, C. Duan, D. W. Kastner, and H. J. Kulik, "MOFSimplify, machine learning models with extracted stability data of three thousand metal–organic frameworks," Sci. Data **9**, 74 (2022).

[234]H. Park, Y. Kang, W. Choe, and J. Kim, "Mining insights on metal–organic framework synthesis from scientific literature texts," J. Chem. Inf. Model. **62**, 1190–1198 (2022).

07 May 2024 15:47:34